Study for the Development of New Anti-Angiogenesis Drugs with VEGF Signal Transduction Inhibitory Activities

（VEGF情報伝達阻害活性を有する新規血管新生抑制剤開発のための研究）

KATSUHIDE IGARASHI

Study for the Development of New Anti-Angiogenesis Drugs with VEGF Signal Transduction Inhibitory Activities

A THESIS SUBMITTED FOR THE DEGREE OF

DOCTOR OF PHILOSOPHY

IN THE UNIVERSITY OF TOKYO

By

KATSUHIDE IGARASHI

December 1998

Contents

Acknowledgment

I express my most sincere gratitude to Professor Koji Yoda, University of Tokyo, for his valuable and continued support, discussion and critical reading of this dissertation. I am indebted to Assistant Professor Harushi Nakajima, University Tokyo, for his valuable suggestions. I appreciate Dr. Naoki Okumura, Head of Advanced Technology Research Laboratories of Nippon Steel Corporation, for the warm and continued support.
I am also indebted to Dr. Isao Uno, Director of Life Science Research Center of Nippon Steel Corporation, Mr. Toshio Isohara and Dr. Toshiaki Kato of Nippon Steel Corporation for their valuable support, discussion and suggestions. I am grateful to Prof. Masabumi Shibuya, University of Tokyo for providing cDNAs of KDR and Flt-1.

I also appreciate Miss Keiko Shigeta of Sanko Corporation for assisting during experimentation throughout the course of this investigation and Miss Tomoka Yamano of Sanko Corporation for constructing several plasmids.

I also thank to Dr. Masamichi Takami of Showa University for his valuable advice and support. I thank the following people of Nippon Steel Corporation: Mr. Shinkichi Kohno, Dr. Yoshio Hayashi, Dr. Jun Katada, Mr. Kaneo Kanoh and Miss Satoko Muramatsu for their valuable comments and suggestions.

Finally, I thank my wife Asako from the bottom of my heart for her support.

Abbreviations

BSA	bovine serum albumin
CH	collagen homology domain
DMEM	Dulbecco's modified Eagle's medium
EGF	epidermal growth factor
EGFR	epidermal growth factor receptor
ELISA	enzyme-linked immunosorbent assay
Flt-1	fms-like tyrosine kinase-1
GAP	GTPase activating protein
Grb2	growth factor binding protein 2
HRP	Horse-radish peroxidase
HUVEC	human umbilical vein endothelial cells
KDR	kinase insert domain-containing receptor
MAPK	mitogen-activated protein kinase
Ni-NTA	nickel affinity chromatography column
PAEC	porcine aortic endothelial cells
PI3K	phosphatidyl inositol 3-kinase
PLCγ	phospholipase C gamma
PTB	phosphotyrosine-binding domain
Sck	Shc-like

SH2	src homology domain 2
SHP-2	src homology 2 phosphatase 2
TCA	trichloroacetic acid
TMBZ	3,3'-5,5'-tetramethylbenzidine
VEGF	vascular endothelial growth factor

Chapter One

Background and literature Review

1-1 Role of angiogenesis in pathological processes

Angiogenesis, the development of new blood vessels, is involved not only in the physiological processes such as embryogenesis and wound healing (Peters et al., 1993), but is also implicated in the pathological processes of a variety of diseases such as diabetic retinopathy, tumors and rheumatoid arthritis (Ferrara, 1995). For example, vision loss in diabetic retinopathy is characterized by extensive formation and proliferation of new blood vessels in the retina (Robinson et al., 1996). The resultant new vessels are directly responsible for various destructive changes such as leakage and bleeding, which are subsequently followed by organization of the clot and fibrosis, and may ultimately lead to retinal detachment or irreversible damage to the macula lutea (Ferrara and Davis-Smyth, 1997). On the other hand, it is well known that the development of new blood vessels within and around the tumor is an important step in the growth of solid tumors in order to provide nutrition and oxygen. This phenomenon is called "tumor angiogenesis" (Fig. 1-1), and previous studies have estimated that tumors with diameter > 2 mm usually show abundant angiogenesis (Folkman, 1995).

Thus, inhibition of angiogenesis might be a promising novel therapy in the above described diseases, since inhibition of tumor angiogenesis should theoretically lead to inhibition of tumor growth and results in the

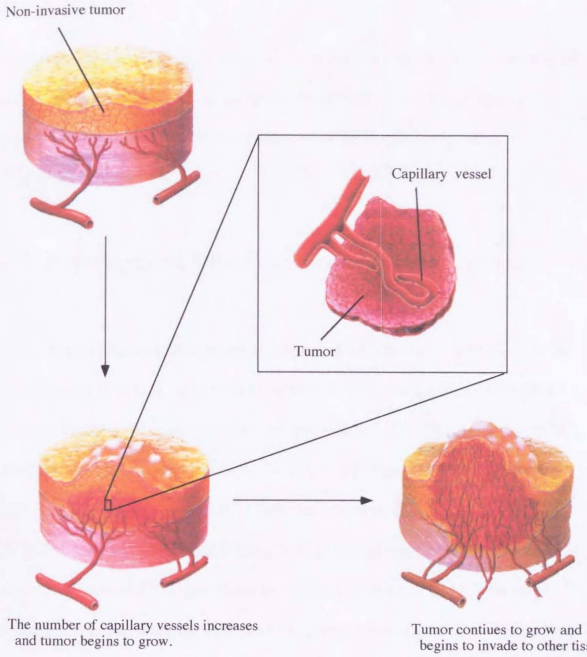

Fig. 1-1 Schematic reprensentation of tumor angiogenesis

This figure was modified from Nikkei Science (1996) vol. 26, no. 12, p.160
Non-invasive tumor turns to invasive tumor. The number of capillary vessels around tumor increases and the tumor begins to grow.
The tumor continues to grow and begins to invade to other tissues.
The figure at upper-right zooms up a capillary vessel in the tumor.

regression or complete resolution of the tumor. To this effect, inhibition of tumor angiogenesis has been recently considered as one of the most promising strategies for the development of new anti-cancer drugs (Folkman, 1995).

1-2 Importance of VEGF in pathological angiogenesis

Several factors that promote angiogenesis have been identified in the last 10 years (Ferrara and Davis-Smyth, 1997). These include epidermal growth factor (EGF), platelet derived growth factor (PDGF) (Pierce et al., 1992), transforming growth factor-α (TGF-α), basic fibroblast growth factor (bFGF) (Hori et al., 1991) and vascular endothelial growth factor (VEGF). Among these, VEGF (Fig. 1-2) is considered to be one of the most important factors. Different from other factors, it has a direct mitogenic activity toward endothelial cells and uniquely shows signal sequence, which is not found in bFGF. In addition, the expression level of VEGF correlated with the pathological condition of many diseases (Ferrara and Davis-Smyth, 1997; Keck et al., 1989; Leung et al., 1989).

VEGF was first reported to be a vascular permeability factor in 1983 by Senger and coworkers. This permeability activity is 100-1,000 times stronger than histamine, which is a well-known vascular permeability factor (Connolly et al., 1989). Therefore, VEGF is also known as the

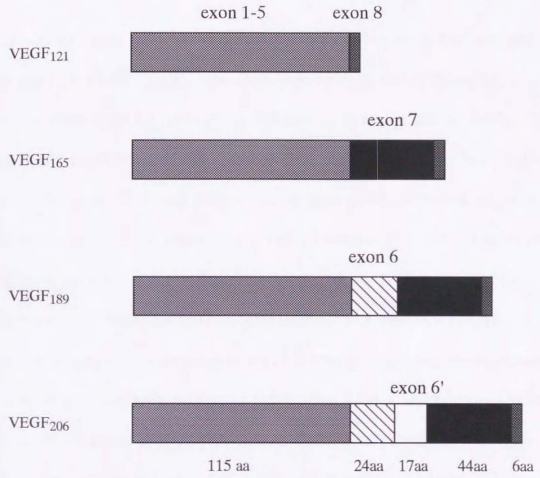

Fig. 1-2 VEGF family

Subtypes of human VEGF. The peptide coded by exon 1-5 represents the "core region" of VEGF, exhibiting the basic level of VEGF activity. Fifty percent of amino acids of the peptide coded by exon 6 is basic amino acids (lysine, arginine). Therefore, this peptide strongly binds to heparin. The peptide coded by exon 7 is rather basic and shows a weak binding to heparin.

"vascular permeability factor (VPF)". On the other hand, Ferrara and Henzel (1989) identified a new angiogenic factor, which showed a mitogenic activity toward bovine endothelial cells and named the factor, vascular endothelial growth factor (VEGF). The cDNAs for both factors were cloned in 1989, and their amino acid sequences revealed that both factors were identical (Keck et al., 1989; Leung et al., 1989). VEGF has a signal sequence and expression of its receptors is virtually restricted to the vascular endothelial cells. The high expression of VEGF is reported in almost all tumors investigated so far, for example, glioblastomas, renal cell carcinomas, neoplastic tumors of the ovaries, kidney and bladder (Berkman et al., 1993; Berse et al., 1992; Brown et al., 1993; Dvorak et al., 1991; Plate et al., 1992; Shweiki et al., 1992; Takahashi et al., 1994). More importantly, tumor differentiation has been shown to correlate well with the extent of VEGF mRNA expression in the case of glioblastoma (Plate et al., 1992). In addition, there is a high correlation between VEGF expression and retinal neovascularization associated with diabetic retinopathy (Aiello et al., 1994). Thus, these findings support the notion that VEGF is one of the most important angiogenic factors.

Several mechanisms are known to be involved in the regulation of VEGF gene expression. Among these, local hypoxia is thought to be the major inducer of expression, thus, VEGF mRNA is highly expressed in ischemic tumor cells that are juxtaposed to areas of necrosis (Shweiki et al.,

1992). Overproduction of VEGF by ischemic retinal cells may promote retinal and iris neovascularization in a number of neovascular eye diseases (Pe'er et al., 1995). Induction of VEGF accompanied by mutation in oncogenes and tumor suppresser genes has also been reported (Arbiser et al., 1997; Kieser et al., 1994; Shweiki et al., 1992). These expression-enhancing mechanisms increase the importance of VEGF in pathological angiogenesis.

It has been shown that the VEGF neutralizing antibody reduced the diameter of the tumor implanted in nude mouse (Kim et al., 1993; Kondo et al., 1993). Furthermore, expression of the VEGF receptor dominant negative form, which has only an extracellular domain, is associated with inhibition of several types of mouse tumors (Millauer et al., 1996; Millauer et al., 1994). Furthermore, antisense oligodeoxynucleotides inhibited retinal neovascularization in a murine model (Robinson et al., 1996). These data indicate that VEGF activity is necessary for these angiogenesis-related pathological processes. Furthermore, they also confirm that inhibition of VEGF activity inhibits pathological angiogenesis.

1-3 VEGF receptors

Three types of receptors for VEGF have so far been described, including KDR, Flt-1 and neuropilin-1 (de Vries et al., 1992; Quinn et al., 1993; Soker et al., 1998) (Fig. 1-3). KDR and Flt-1 are tyrosine kinase type

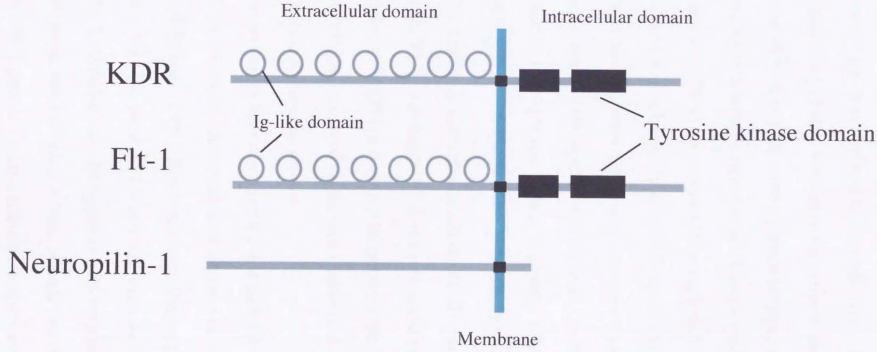

Fig. 1-3 Three VEGF receptors

There are three receptors for VEGF, KDR, Flt-1 and Neuropilon-1.
KDR and Flt-1 are tyrosine kinase type receptors and closely related to each other.
They have seven immunogloblin (Ig)-like domains in their extracellular domains.

receptors and are closely related to each other (Fig. 1-4). Both have seven immunoglobulin (Ig)-like domains in the extracellular domain (ECD), a single transmembrane region and a consensus tyrosine kinase sequence that is interrupted by a kinase-insert domain. Their amino acid sequence homologies are 32% in their extracellular regions, 78% in their amino halves of the tyrosine kinase domain, 51% in their kinase insert domains and 78% in their carboxyl halves of the tyrosine kinase domain (Shibuya, 1995). Flt-1 has the highest affinity for $VEGF_{165}$, with a Kd of approximately 10-20 pM (de Vries et al., 1992). KDR has a somewhat lower affinity for VEGF; its Kd is approximately 75-125 pM (Terman et al., 1992). Neuropilin-1, a recently identified VEGF receptor, has been shown to modulate VEGF binding to KDR and subsequent bioactivity, its coexpression with KDR in certain cells enhances the binding of $VEGF_{165}$ to KDR and $VEGF_{165}$-mediated chemotaxis (Soker et al., 1998). Whether it signals itself is not clear at present.

Recent studies have demonstrated that both Flt-1 and KDR are essential for the normal development of embryonic vasculature (Fong et al., 1995; Shalaby et al., 1995). Mouse embryos homozygous for a targeted mutation in the Flt-1 locus died *in utero* between days 8.5 and 9.5 (Fong et al., 1995). Endothelial cells developed in both embryonic and extraembryonic sites but failed to form normal vascular channels. Mice in which the Flk-1 gene had been inactivated lacked vasculogenesis and also

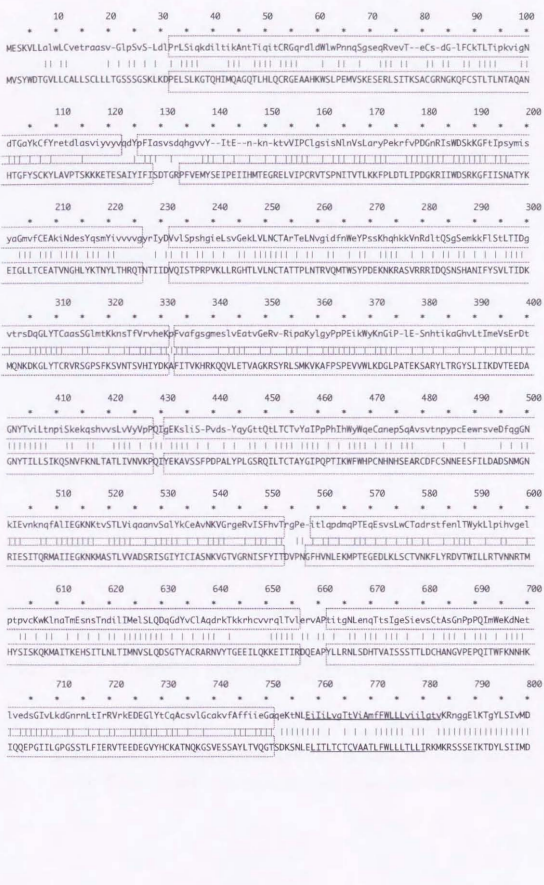
KDR
Flt-1
MESKVLLalwLCvetraasv-GlpSvS-LdlPrLSiqkdiltikAntTiqitCRGqrdldWlwPnnqSgseqRvevT--eCs-dG-lFCkTLTipkvigN
MVSYWDTGVLLCALLSCLLLTGSSSGSKLKDPELSLKGTQHIMQAGQTLHLQCRGEAAHKWSLPEMVSKESERLSITKSACGRNGKQFCSTLTLNTAQAN
dTGaYkCfYretdlasviyyvvqdYpFIasvsdqhgvvY--ItE--n-kn-ktvVIPClgsisNlnVsLaryPekrfvPDGnRIsWDSkKGFtIpsymis
HTGFYSCKYLAVPTSKKKETESAIYIFISDTGRPFVEMYSEIPEIIHMTEGRELVIPCRVTSPNITVTLKKFPLDTLIPDGKRIIWDSRKGFIISNATYK
yaGmvfCEAkiNdesYqsmYivvvvgyrIyDVvlSpshgieLsvGekLVLNCTArTeLNvgidfnWeYPssKhqhkkVnRdltQSgSemkkFlStLTIDg
EIGLLTCEATVNGHLYKTNYLTHRQTNTIIDVQISTPRPVKLLRGHTLVLNCTATTPLNTRVQMTWSYPDEKNKRASVRRRIDQSNSHANIFYSVLTIDK
vtrsDqGLYTCaasSGlmtKknsTfVrvheKpFvafgsgmeslvEatvGeRv-RipaKylgyPpPEikWyKnGiP-lE-SnhtikaGhvLtImeVsErDt
MQNKDKGLYTCRVRSGPSFKSVNTSVHIYDKAFITVKHRKQQVLETVAGKRSYRLSMKVKAFPSPEVVWLKDGLPATEKSARYLTRGYSLIIKDVTEEDA
GNYTvILtnpiSkekqshvvsLvVyVpPQIgEKsliS-Pvds-YqyGttQtLTCTvYaIPpPhIHWyWqeCanepSqAvsvtnpypcEewrsveDfqgGN
GNYTILLSIKQSNVFKNLTATLIVNVKPQIYEKAVSSFPDPALYPLGSRQTLTCTAYGIPQPTIKWFWHPCNHNHSEARCDFCSNNEESFILDADSNMGN
kIEvnknqfAlIEGKNKtvSTLViqaanvSalYkCeAvNKVGrgeRvISFhvTrgPe-itlqpdmqPTEqEsvsLwCTadrstfenlTWykLlpihvgel
RIESITQRMAITEGKNKMASTLVVADSRISGIYICIASNKVGTVGRNISFYITDVPNGFHVNLEKMPTEGEDLKLSCTVNKFLYRDVTWILLRTVNNRTM
ptpvcKwKlnaTmEsnsTndilIMelSLQDqGdYvClAqdrkTkkrhcvvrqlTvlervAPkitgNLenqTtsIgeSievsCtAsGnPpPQImWeKdNet
HYSISKQKMAITKEHSITLNLTIMNVSLQDSGTYACRARNVYTGEEILQKKEITIRDQEAPYLLRNLSDHTVAISSSTTLDCHANGVPEPQITWFKNNHK
lvedsGIvLkdGnrnLtIrRVrkEDEGlYtCqAcsvlGcakvfAffiieGqqeKtNLEiTiLvqTtViAmfFWLLLviilgtvKRnggElKTgYLSIvMD
IQQEPGTILGPGSSTLFIERVTEEDEGVYHCKATNQKGSVESSAYLTVQGTSDKSNLELITLTCTCVAATLFWLLLTLIRKMKRSSSEIKTDYLSIIMD

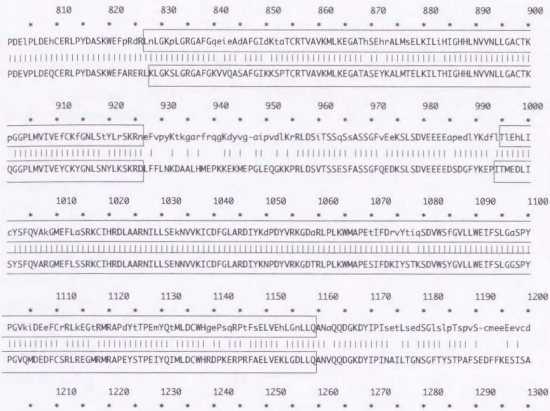

Fig. 1-4 Alignment of human KDR with Flt-1

Flt-1 amino acid number is shown.

Identical or closely related amino acids are marked with vertical lines.

Ig-like domains are shown within dotted boxed areas, transmembrane regions are underlined while boxed areas represent tyrosine kinase domains.

Angiogenesis inhibitor	Inhibition of the growth of endothelial cell	Inhibition of in vivo angiogenesis
(1) Microorganic metabolites		
Fumagilin	+	+
AGM1470	+	+
FR118487	+	+
DS4152	+	+
Suramin	+	+
(2) Neutralizing antibodies		
Anti-integrin$\alpha_v\beta_3$	+	+
Anti-basic FGF	+	+
Anti-VEGF	+	+
(3) Proteins		
Platelet factor IV	+	+
CDI[1)]	+	+
TIMP[2)]	+	+
TSP	+	+
TGF-β	+	-
TNF-α	+	-
Angiostatin	+	+
Endostatin	+	+
(4) Others		
Protamin	+	+
Angiostatic steroid	+	+
Vitamin A derivative	+	+
Vitamin D3 derivative	+	+

Table 1-1 Angiogenesis inhibitors and their effects

Modified from Kodansha (1997). Chorioallantoic membrane assay (CAM) or rabbit cornea assay were used to monitor the inhibitory activity of the compounds on angiogenesis in vivo.

[1]CDI: cartilage derived inhibitor.
[2]TIMP: tissue inhibitor of proteinase.

failed to develop blood islands. Furthermore, hematopoietic precursors were severely disrupted and organized blood vessels failed to develop throughout the embryo or yolk sac, resulting in death *in utero* between days 8.5 and 9.5 (Shalaby et al., 1995).

1-4 Inhibitors of angiogenesis

Table 1-1 lists various angiogenic inhibitors reported so far in the literature. These inhibitors are classified into the following three broad categories. *(1)* Microorganic metabolites whose inhibitory mechanisms are almost unknown at present. *(2)* Neutralizing antibodies against various angiogenic factors. *(3)* Proteins whose inhibitory mechanisms are almost not clear at present.

Recent studies have indicated that Angiostatin and Endostatin, which are categorized as protein inhibitors of angiogenesis, are the most attractive factors (Zetter, 1998). Angiostatin is the fragment of plasminogen and Endostatin is the fragment of collagen. Furthermore, Angiostatin and Endostatin have also been shown experimentally to reduce the size of four types of tumors implanted in mice (Mauceri et al., 1998) thus making them more attractive for clinical use.

1-5 The purpose of this study

The aim of the present study was to develop new agents that inhibit the growth of tumors by arresting angiogenesis. Based on the above background, I defined the following two properties as essential features of new anti-angiogenesis drugs:

(1) Small molecule compounds rather than proteins.

(2) Known mechanism of inhibition of angiogenesis.

In the first part of this study, I searched for small-molecule inhibitors of VEGF signal transduction. To inhibit VEGF signal transduction, two strategies are available at present.

(1) Intracellular inhibition, i.e., inhibition of VEGF downstream signal transduction.

(2) Extracellular inhibition, i.e., inhibition of VEGF binding to its receptors. However, information about the mechanism of VEGF downstream signal transduction is limited at present. Therefore, for the first strategy, I first searched for unidentified proteins that bind to KDR and Flt-1. I believe that there might be endothelial-specific proteins that bind to the cytoplasmic regions of KDR and Flt-1, and that such agents will be promising specific inhibitors of VEGF signal transduction. For the

second strategy, I screened my chemical library for inhibitors of the binding of VEGF to its receptor, KDR.

Chapter 2

Analysis of proteins binding to Flt-1 and KDR

2-1 Introduction

At present, very little is known about the signal transduction of VEGF (Fig. 2-1) compared with that of EGF and PDGF. In EGF and PDGF system, the proteins that bind to receptors, the domains to which they bind to, and their importance to signal transduction have been well characterized. In comparison, only a few proteins that form a complex with VEGF receptors have been identified, making it very difficult to explain the diversity of VEGF-induced cellular responses. Therefore, in the first part of this study, I attempted to define the basic aspects of VEGF signal transduction in order to determine the potential targets for VEGF inhibitors.

Binding of VEGF to its receptors, KDR and Flt-1, induces autophosphorylation of their tyrosine residues (Waltenberger et al., 1994). The phosphorylated receptors are thought to recruit proteins with SH2 domains or phospho-tyrosine-binding domains to their phosphorylated tyrosine residues and transduce the downstream signal transduction. Immunological studies suggested that PI3K p85, PLCγ, Nck and GAP bind to both Flt-1 and KDR in bovine aortic endothelial cells (Guo et al., 1995). Using the baculovirus expressed Flt-1 as a probe, PLCγ has been shown to bind to the phosphorylated Y1169 of Flt-1 (Sawano et al., 1997). The yeast two hybrid analysis revealed that both N- and C-SH2 domains of PI3K p85

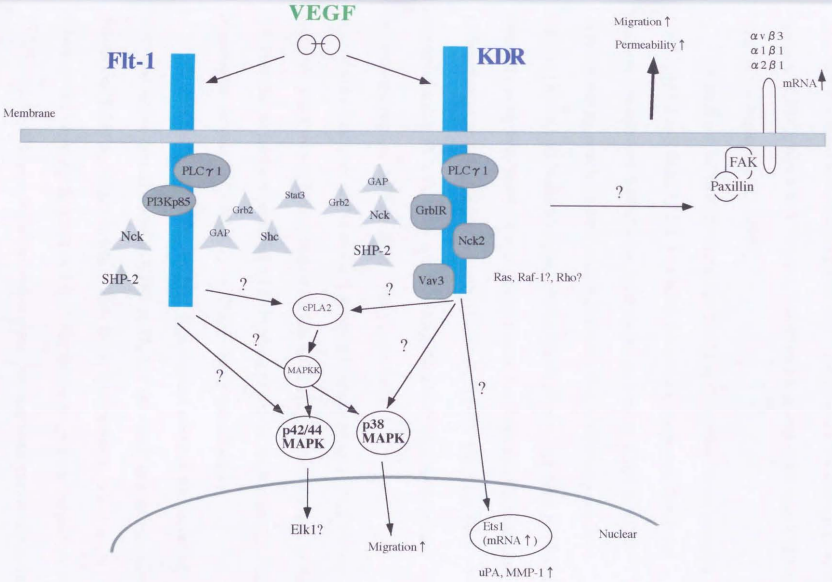

Fig. 2-1 VEGF intracellular signal transduction

bind to Y1213 of Flt-1 (Cunningham et al., 1995) while N- but not C-SH2 domain of PLCγ binds to Y794 and Y1169 of Flt-1 and Y801 and Y1175 of KDR (Cunningham et al., 1997).

In addition to these proteins, the bindings of another three proteins, Grb2, SHP-2 and Stat3 to Flt-1 or KDR have been suggested. Grb2 and tyrosine phosphatase SHP-2 have been shown to bind to KDR in KDR-overexpressing porcine aortic endothelial cells in a VEGF-dependent manner (Kroll and Waltenberger, 1997). Whether they also bind to Flt-1 is currently unknown. Stat3, a transcription factor, has recently been reported to function as an adapter protein. (Pfeffer et al., 1997). Flt-1 has the consensus motif (YXXQ) for Stat3 binding (Stahl et al., 1995) in its cytoplasmic region (YSFQ; 1002 - 1005 amino acids).

In the first part of the study, I screened human brain cDNA library using the yeast two-hybrid system with the KDR cytoplasmic domain as the bait in order to find unidentified KDR binding proteins. Such proteins will be potential targets for inhibitors of VEGF signal transduction.

In the second part of the study, I investigated whether the proteins described above directly bind to KDR or Flt-1. I also analyzed the tyrosine residues of KDR and Flt-1 to which they bind. The proteins, which were shown to bind directly to KDR or Flt-1, can be the targets for inhibitors of VEGF signal transduction. Information about the sequence surrounding the

tyrosine residues to which they bind may be helpful for the design of peptide mimetic inhibitors that selectively inhibit their binding.

2-2 Sck interacts with KDR and Flt-1 via its SH2 domain

2-2-1 Materials and Methods

Yeast two-hybrid system screen

Flt-1 and KDR cDNA were kindly provided by Dr. M. Shibuya (Department of Genetics, Institute of Medical Science, University of Tokyo). The cytoplasmic domains of KDR (788-1354 amino acids) and Flt-1 (781-1338 amino acids) were amplified by PCR and subcloned into the yeast two hybrid plasmid pGBT9 (Clontech, Paolo Alto, CA) and used as bait plasmids (KDR/pGBT9 and Flt-1/pGBT9). A human brain cDNA library constructed in prey plasmid pACT2 and pretransformed into the yeast strain Y187 (*MATα, ura3-52, his3-200, ade2-101, trp1-901, leu2-3, 112, gal4Δ, gal80Δ, met⁻, URA3 :: GAL1*$_{UAS}$*-GAL1*$_{TATA}$*-lacZ)* was purchased from Clontech. Screening was performed as described in the instructions provided by the manufacturer. Briefly, yeast PJ69-2A (*MATa, trp1-901, leu2-3, 112, ura3-52, his3-200, gal4Δ, gal80Δ, LYS2::GAL1*$_{UAS}$-

GAL1$_{TATA}$*-HIS3, GAL2*$_{UAS}$*-GAL2*$_{TATA}$*-ADE2)* transformed with KDR/pGBT9 was mated with yeast Y187 pretransformed with the library. The resultant diploids were selected as colonies growing without adenine and histidine. β-galactosidase activity of each colony was assayed and colonies showing positive activities were selected. Library plasmids were isolated from selected colonies and re-introduced into the yeast Y187 to confirm interaction with KDR cytoplasmic region. Positive clone cDNAs were partially sequenced.

Construction of Sck mutants

Partial Sck cDNA was isolated by using the Rapid-Screen cDNA Library Panel human fetal brain (OriGene). Briefly, master 96 well plate was screened by PCR with the primer pair, Sck/SH2/FW (TTCCCTTGGAGGACCACTGG) and Sck/SH2/RV (AGGCGAAATGGTTCCGTCTTTGG). Nine sub-plates corresponding to wells showing positive amplification were re-screened by PCR with the same primer pair. *Escherichia coli* cells in positive wells were isolated and screened with the same primer pair. Candidate clones were sequenced and the clone (8B6A5) containing the PTB domain was isolated.
Partial Sck constructs used here were prepared by PCR and subcloned into the prey vector pACT2. Primer pairs were: sense 5' - GGAATTCGATTCATCCGGAAGGGCAGCTTCATCC-3', antisense 5' -

CCGCTCGAGTCAGGGCTCCCGTGAGACCACG- 3' for plasmid containing PTB, CH and SH2 domains (Sck PTB-CH-SH2); sense 5' - GGAATTCGATTCATCCGGAAGGGCAGCTTCATCC-3', antisense 5' - CCGCTCGAGCGGGATGCTGTTGTAGTAATTGTG- 3' for plasmid containing PTB domain (Sck PTB); sense 5' - GAAGATCTTTCCCTTGGAGGACCAGTGG-3', antisense 5' - CCGCTCGAGGCGAAATGGTTCCGTCTTTGG- 3' for plasmid containing SH2 domain (Sck SH2). For plasmid containing PTB and CH but not SH2 domains (Sck PTB-CH), plasmid Sck PTB-CH-SH2 was digested with *Pvu*II and *Xho*I. The fragment containing the vector sequence was blunt ended and ligated.

Construction of Flt-1 and KDR mutants

Site-directed mutagenesis of KDR was carried out using the Chameleon double-stranded site-directed mutagenesis kit (Stratagene, La Jolla, CA). The sequences of mutating primers were as follows:
Y801F, AACTGAAGACAGGCTTCTTGTCCATCGTCATGG;
Y822F, GTGAACGACTGCCTTTTGATGCCAGCAA;
K868A, GGACAGTAGCAGTCGCAATGTTGAAAGAAGG;
Y951F, AGGGAAAGACTTCGTTGGAGCAATCC;
Y996F, CCTGAAGATCTGTTTAAGGACTTCCTGACC;
Y1175F, GGATGGCAAAGACTTCATTGTTCTTCCG;

Y1319F, CAGACACCACCGTGTTCTCCAGTGAGGAAGC.

Site-directed mutagenesis of Flt-1 was carried out using the same kit. Mutating oligonucleotides were synthesized as follows:

Y794F,GAAATAAAGACTGACTTCCTATCAATTATAATGGACCC ;

Y815F, GTGAGCGGCTCCCTTTTGATGCCAGCAAGTG ;

K861A, GGACTGTGGCTGTCGCGATGCTGAAAGAGG ;

Y990F, TTCTGACGGTTTCTTCAAGGAGCCC ;

Y1169F, CAACAGGATGGGAAAGACTTCATCCCAATC ;

Y1184F, ATAGTGGGTTTACATTCTCAACTCCTGCCTTC ;

Y1213F,GGAAGCTCTGATGATGTAAGATTTGTGAATGCTTTCAAG ;

Y1242F, CCATGTTTGATGACTTCCAGGGCGACAGC ;

Y1309F, GCGCAGGTTCACCTTCGACCACGCTGAG ;

Y1327F, CCGCCCCCAGACTTCAACTCGGTGGTCC ;

Y1333F, CTCGGTGGTCCTGTTCTCCACCCCACCCATC.

The triple mutant of Flt-1 (Y1309F, Y1327F and Y1333F) was constructed with three primers, Y1309F, Y1327F and Y1333F.

β-Galactosidase assay

The filter assay was performed according to the method of Bartel et al. (Bartel et al., 1993). Briefly, transformants were streaked directly on a nylon membrane placed on $Leu^-Trp^-His^+$ plate and incubated at 30°C for 24

h. The filter was then transferred into liquid nitrogen for 20 s and allowed to thaw at room temperature then placed on a paper filter that was presoaked in Z buffer/X-Gal solution (22.2 g/L $Na_2HPO_4 \cdot 12H_2O$, 5.9 g/L $NaH_2PO_4 \cdot 2H_2O$, 0.75 g/L KCl, 0.246 g/L $MgSO_4 \cdot 7H_2O$, and 390 mg/L X-Gal) and incubated at 30°C for about 8 hr. Liquid culture assays using a chemiluminescent substrate (Galacton Plus (Roche Molecular Biochemicals) for the quantification of β-galactosidase activity were performed according to the method described in the Yeast Protocols Handbook (Clontech). Briefly, the transformants were grown to saturation in $Leu^-Trp^-His^+$ medium overnight then diluted the following morning. Diluted yeasts were grown to an optical density (A_{600}) of about 0.6 and pelleted. Yeasts were washed in Z buffer once and resuspended in 300 μl Z buffer and placed in liquid nitrogen until frozen. At a later stage, yeasts were thawed by incubation in a 37°C water bath for 1 min. This freeze/thaw cycle was repeated once and the yeast lysate was centrifuged for 5 min. Yeast supernatants were collected and used as yeast extract. Enzymatic reactions and light measurements were performed according to the protocol recommended by the manufacturer.

RT-PCR analysis

5×10^5 human umbilical vein endothelial cells (HUVEC) (primary culture, passage number 3, (Kurabou) grown in HuMedia-EG2 (Kurabou)

were used as the source of mRNAs. mRNAs were purified using the mRNA capture kit (Roche Molecular Biochemicals). RT-PCR was performed using Titan one tube RT-PCR system (Roche Molecular Biochemicals) with either the Sck specific primer pair, Sck/P/F4 (AGAGCAACCTTCGCTTTGCC) and Sck/P/B9 (AGGGTCGCATGTCAAACAGATC) or the human β-actin specific primer pair, β-AC/FW (CCAAGGCCAACCGCGAGAAGATGAC) and β-AC/RV (AGGGTACATGGTGGTGCCGCCAGAC). All procedures were performed according to the instructions provided by the manufacturer.

2-2-2 Results and Discussion

Identification of Sck as a binding protein of KDR

I screened human brain cDNA library using the yeast two-hybrid system with KDR cytoplasmic region as the bait. As a screening method, I used diploids grown without adenine and histidine, which were constructed from mating yeast PJ69-2A that expressed KDR with yeast Y187 expressing the library (Fig. 2-2). Yeast PJ69-2A has two reporter genes, *ADE2* and *HIS3*, therefore, yeasts having a cDNA for KDR binding proteins are also able to grow without adenine and histidine. After two rounds of screening, I obtained 50 colonies that were able to grow in adenine- and histidine-free environment, among 6.2×10^6 diploids. In order to remove false positives,

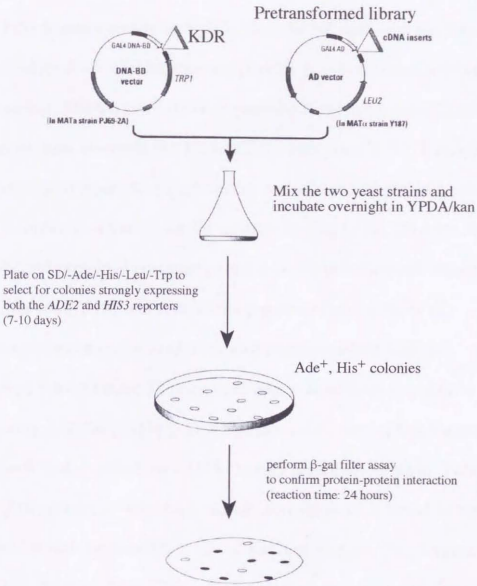

Fig. 2-2 Procedure used for the yeast two-hybrid system screening of pretransformed cDNA libraries.

Reproduced from the Product Protocol provided by Clontech Laboratories, Inc. and modified according to the actual conditions of the screening used in the present study.

I assayed the β-galactosidase activity in these 50 colonies with the filter assay and selected 48 colonies showing positive β-galactosidase activity. After isolating cDNA library-derived plasmids from these yeasts, I co-transformed these plasmids and KDR/pGBT9 into yeast Y187. I assayed β-galactosidase activity of the transformants and selected 38 plasmid clones. Finally, in order to select clones for protein binding to the DNA binding region of Gal4 protein, I co-transformed these 38 plasmids and vector pGBT9 into yeast Y187 and assayed the β-galactosidase activity of transformants, but none showed a positive β-galactosidase activity. Therefore, I selected these 38 plasmid clones as candidates for cDNAs of KDR binding proteins (Table 2-1). I determined the partial DNA sequences of the inserts and searched for cDNAs having homology to them. Table 2-2 is a list of the results of homology search. Among these, I found a fragment of Sck gene (clone number 2#7), one of Shc homologues. This fragment contained nucleotide 616 to 2356 of the partial sequence of Sck cDNA described by Nakamura et al. (Nakamura et al., 1998) (Fig. 2-3). Analysis of porcine aortic endothelial cell (PAEC) overexpressing KDR showed that Shc forms a complex with KDR in a VEGF stimulation-dependent manner and becomes phosphorylated on its tyrosine residues (Kroll and Waltenberger, 1997). These data suggest that Sck might also play a role in KDR signal transduction in endothelial cells through binding to KDR. Therefore, I selected Sck for further analysis.

Total diploids	6.2×10^6
Ade^+, His^+ colonies	50
β-gal positive	48
Confirmation by retransformation of prey plasmid	
bait-dependent	38
vector-dependent	0

Table 2-1 Results of screening for KDR binding proteins.

The numbers of colonies or clones are shown. Ade+, His+ colonies represent the number of colonies that can grow on agar medium without adenine and histidine. β-gal positive represent the number of colonies that show reasonable strength of blue color in β-gal filter assay.
Bait -dependent represents the number of clones that reproduced the positive reults with KDR bait plasmid. Vector-dependent represents the number of clones that show the positive resultswith empty vector bait plasmid.

Total number of clones	38
ATP synthase	4
nucleolar protein	2
PI3K p85	11
Shc	3
none	18

Table 2-2. Results of homology search of inserts.

Partial DNA sequence of clones inserts was determined and the homology search was performed using FASTA program on March 30, 1998.

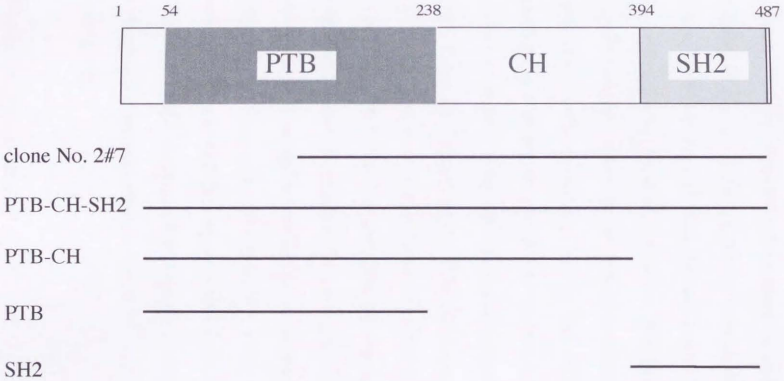

Figure 2-3. Wild type and mutant Sck.

PTB and SH2 domains are indicated by shaded boxes.

Clone segments analyzed in the present study are indicated by bars.

Twelve clones (clone number 1#7, 1#10, 1#11, 1#13, 1#35, 2#1, 2#2, 2#8, 2#10, 2#13, 2#14, 2#19) were highly homologous to PI3K p85, the regulatory subunit of phosphatidyl inositol 3-kinase. In section two of this chapter (see Fig. 2-11), I could not detect the binding of N- and C-SH2 domains of PI3K p85 to KDR by the yeast two hybrid analysis (Igarashi et al., 1998). This discrepancy might be due to differences in the expression level of PI3K p85. I used the low-level expression vector pGAD424 in section two; on the other hand, I used the high-level expression vector pACT2 in screening studies. PI3K p85 has been shown to bind to Flt-1 cytoplasmic region by the yeast two hybrid analysis (Cunningham et al., 1995). It has also been shown that PI3K p85 forms a complex with KDR and Flt-1 in bovine aortic endothelial cells (BAEC) upon VEGF stimulation (Guo et al., 1995). The result that PI3K p85 was selected through screening with KDR cytoplasmic region as the bait suggests that PI3K p85 might play some role in VEGF signal transduction by binding to KDR as well as Flt-1. However, previous studies have shown that VEGF stimulation in endothelial cells failed to activate PI3K enzymatic activity (Abedi and Zachary, 1997). Therefore, further analysis will be required to determine the role of PI3K p85 in VEGF signal transduction. The remaining 25 clones are now under investigation.

Expression of Sck in HUVEC

If Sck plays some role in VEGF signal transduction, its expression in endothelial cells must be confirmed. Recent studies have shown that Sck is expressed mainly in human liver, pancreas and prostate (Nakamura et al., 1998). However, to my knowledge, its expression in endothelial cells has not yet been reported. Therefore, I performed RT-PCR analysis using specific primers for Sck (corresponding to 509-1189 of AB001451) to determine the expression of Sck mRNA in endothelial cells. I purified mRNA from HUVEC and used it as the template. Figure 2-4 shows that a band with an expected length, i.e., 681 bp, was amplified with the Sck specific primer. These results indicate that that Sck is expressed in endothelial cells.

Sck interacts with both KDR and Flt-1 and their interaction is kinase-dependent

I also tested whether Sck binds to KDR and Flt-1. Using plasmid Flt-1/pGBT9 to express Flt-1 cytoplasmic region as the bait, I assayed β-galactosidase activity of each transformant. As shown in Fig. 2-5, Sck bound to Flt-1 as well as to KDR. Next, I examined whether such binding was dependent on tyrosine kinase activity of KDR and Flt-1 using mutants without kinase activity. As shown in Fig. 2-5, the binding of Sck to KDR and Flt-1 was totally dependent on kinase activity. These results suggest that

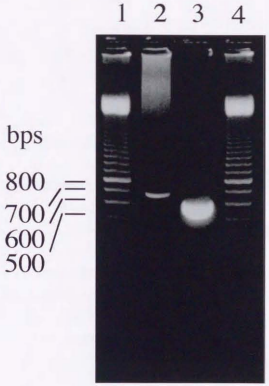

Fig. 2-4 Expression of Sck mRNA in HUVEC.

mRNA purified from 5 x 10^5 HUVECs grown in growth media were subjected to the RT-PCR using the primer pairs for Sck *(lane2)* and β-actin *(lane3)*. 100 bp DNA size markers were loaded at both sides *(lane 1 and 4)*. Similar results were obtained in three different experiments.

A

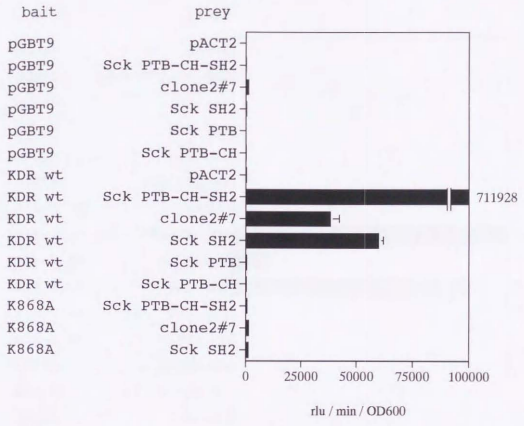

Fig. 2-5A Sck binds to KDR via its SH2 domain.

Baits were cytoplasmic regions of wild type and kinase mutant of KDR (above) and Flt-1 (next page) introduced into pGBT9. Preys were mutants of Sck introduced into pACT2.The bait and prey plasmids were cotransformed into the yeast reporter strain Y187. Liquid assay of β-galactosidase activity of the transformants was assayed using chemiluminescent Galacton Start as a substrate. Values represent the mean ± SD of triplicate determinations expressed in relative light units divided by reaction time (60 min) and optical density.

B

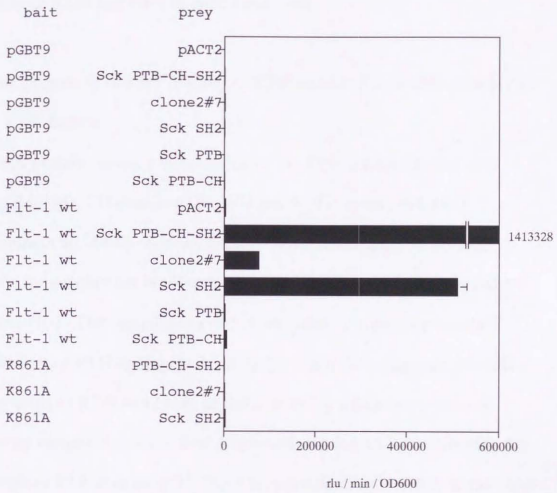

Fig. 2-5B Sck binds to Flt-1 via its SH2 domain.

See legend of figure 2-5A.

Sck binds to the phosphorylated tyrosine residues of KDR and Flt-1 upon activation of KDR and Flt-1 in endothelial cells.

Essential domain of Sck for binding to KDR and Flt-1 is its SH2 domain but not its PTB domain

Sck protein contains three domains, i.e. PTB domain (amino acid number 54-238), CH domain (239-393) and SH2 domain (394-487) (Nakamura et al., 1998). Among these domains, PTB and SH2 domains might be responsible for binding to phosphorylated tyrosine residues of KDR and Flt-1. The partial clone of Sck obtained by screening has the C terminal half of PTB domain and full SH2 domain. This suggests that SH2 domain binds to KDR and Flt-1. In order to construct the prey plasmid expressing various regions of Sck, I obtained a cDNA of Sck containing the full length of PTB domain (193-2356) from human brain cDNA library and used it as a template for PCR. I first investigated whether SH2 domain of Sck can bind to KDR and Flt-1. β-galactosidase activity of each transformant was quantified using Galacton-Star as a substrate. As shown in Fig. 2-5, SH2 domain could bind to both KDR and Flt-1. Next, I examined whether the PTB domain binds to KDR and Flt-1. The results showed that PTB domain could not bind to KDR or Flt-1. In addition, the clone containing full PTB domain and SH2 domain bound to both KDR and Flt-1 while the clone containing full PTB domain but not SH2 domain could not

bind to them. Combined together, these results indicated that the SH2 domain of Sck is an essential region for its binding to KDR.

Unexpectedly, the β-galactosidase activities of transformants with Sck PTB-CH-SH2 were much higher than those of other transformants. This suggests that although PTB domain and CH domain are not necessary for the binding of Sck to KDR and Flt-1, they may be important for the stabilization of SH2 domain structure, thus allowing a firm binding. However, further studies must be conducted to confirm this possibility.

Sck SH2 domain binds to Y1175 of KDR

To determine the tyrosine residues of KDR and Flt-1 responsible for Sck binding, I co-transformed the SH2 domain of Sck and either KDR or Flt-1 mutant constructs whose tyrosine residues were individually mutated to phenylalanine (Fig. 2-6). β-galactosidase activity of each transformant was quantified using Galacton-Star as substrate. As shown in Fig. 2-5, mutations of kinase domain (K868A of KDR and K861A of Flt-1) caused a complete loss of activity. Substitution of Y1175 of KDR resulted in a loss of about 98% of β-galactosidase activity (Fig. 2-7). However, substitution of tyrosine residues of Flt-1 did not cause a significant loss of β-galactosidase activity (data not shown). These results indicate that Y1175 of KDR is responsible for the binding to Sck. I also examined the effect of a triple mutant of Flt-1 (Y1309F, Y1327F and Y1333F), however, it did not lead to

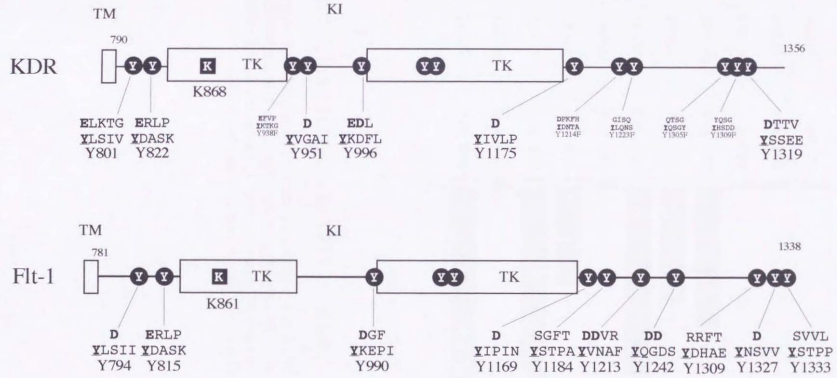

Fig. 2-6 Schematics of KDR and Flt-1 cytoplasmic regions.

Shown are mutated tyrosine residues used in this study.

TM, transmembrane; KI, kinase insert; TK, tyrosine kinase

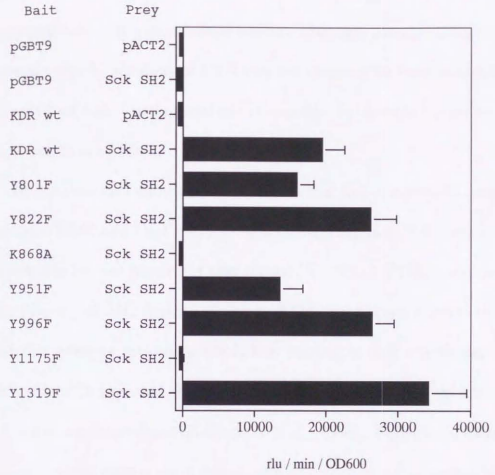

Fig. 2-7. Sck SH2 binds to Y1175 of KDR.

The prey Sck SH2 plasmid was co-transformed with KDR mutants into yeast Y187. β-galactosidase activity of resultant transformants was assayed using chemiluminescent Galacton Star as a substrate. Values represent the mean ± SD of triplicate determinations expressed in relative light units divided by reaction time (60 min) and optical density.

a significant loss of β-galactosidase activity (data not shown). There might be several tyrosine residues of Flt-1 that are responsible for the binding to SH2 domain of Sck. Further analysis is required to identify the responsible tyrosine residues of Flt-1.

In conclusion, I showed in this section that Sck is a protein that binds to activated KDR and Flt-1 and that SH2 domain but not PTB domain of Sck is responsible for the binding. I also showed Y1175 of KDR is responsible for the binding of SH2 domain of Sck to KDR, but I could not determine the responsible tyrosine residue of Flt-1. The binding of Sck to activated EGFR has been recently reported, however, the responsible tyrosine residues of EGFR were not determined (Nakamura et al., 1998). Therefore, this is the first time that the surrounding amino acid sequence of tyrosine residues to which Sck binds has been identified.

What is the role of Sck in VEGF signal transduction? Recent studies by Nakamura and colleagues (Nakamura et al., 1998) have shown that upon EGF stimulation, Sck binds to EGFR and is phosphorylated on the receptor tyrosine residues and Grb2 then binds to the phosphorylated Sck. Therefore, Sck might play a role in the activation of mitogen-activated protein kinase (MAPK) as an adapter protein in EGF system. It is possible that Sck might also play a similar role in VEGF system. Further studies such as investigation of the effect of antisense repression of Sck, are necessary to determine the role of Sck in VEGF signal transduction.

2-3 Tyrosine 1213 of Flt-1 is the Major Binding Site of Nck and SHP-2.

2-3-1 Materials and Methods

Yeast two-hybrid system

Vector plasmids (pGBT9 and pGAD424), yeast hosts SFY526 (MATa, ura3-52, his3-200, ade2-101, lys2-801, trp1-901, leu2-3, 112, can^r, gal4-542, gal80-538, URA3 :: $GAL1_{UAS}$-$GAL1_{TATA}$-lacZ) and Y190 (MATa, ura3-52, his3-200, ade2-101, lys2-801, trp1-901, leu2-3, 112, gal4Δ, gal80Δ, cyh^{r}2, LYS2 :: $GAL1_{UAS}$-$HIS3_{TATA}$-HIS3, URA3 :: $GAL1_{UAS}$-$GAL1_{TATA}$-lacZ) were purchased from Clontech. Yeast two-hybrid plasmid pGBT9 containing the cytoplasmic region of KDR (790-1356 amino acids); (KDR/pGBT9) and Flt-1 (781-1338 amino acids); (Flt-1/pGBT9), indicated in section 2-2-1, was used as the bait. Partial cDNAs (containing SH2 region) of PLCγ, PI3K p85, Nck, Grb2, SHP-2, Stat3 and GAP were cloned by PCR from human placenta cDNA library (Clontech) and their sequences were confirmed by DNA sequencing. Their SH2 domains were PCR amplified and subcloned into pGAD424 and used as prey plasmids. Primer pairs are listed in Table 2-3. The resultant bait and prey plasmids were co-transformed into SFY526 or Y190 yeast hosts.

domain		*5'→3'*
N-SH2 of PLCγ	sense	AGTGCGAATTCAATGAGAAGTGGTTCCATGGG
	antisense	ATAAGTCGACGCTGTGGGACAGGCTCTGAAAG
C-SH2 of PLCγ	sense	AGTGCGAATTCCCACGAGAGCAAAGAGTGGTAC
	antisense	ATAAGTCGACGCTCCTCGTTGATGGGATAGCG
N-SH2 of PI3K p85	sense	GCGAATTCCCTACTACTGTAGCCAACAACGGT
	antisense	CGGCGTCGACGGTATTTGGATACTGGATAAAG
C-SH2 of PI3K p85	sense	GCGAATTCGATGAAGATTTGCCCCATCATGATGAG
	antisense	CCAGAGTCGACTTCATCGCCTCTGCTGTGCATATACTG
SH2 of Nck	sense	GCGAATTCAGGCCTTCACTCACTGGAAAGTTTGC
	antisense	CCAGAGTCGACGGTCAGCAGTATCATGATAAATGCTTGACAAG
SH2 of Grb2	sense	CCGAATTCGTCCTTTTTTGGCAAAATCC
	antisense	TACGGTCGACTTAGGCTGCTGTGGCACCTGTTC
N-SH2 of SHP-2	sense	CCGAATTCATGACATCGCGGAGAT
	antisense	TACGGTCGACTTATGCACAGTTCACACCATATTTAAGC
C-SH2 of SHP-2	sense	CCGAATTCTGGTTTCATGGACATCT
	antisense	TACGGTCGACTTACTTGAGTTGTAGTACTGTACCC
SH2 of Stat3	sense	AGTGCGAATTCATTGGAACCTGGGACCAAGTGGC
	antisense	ATAAGTCGACTCACATGGGGGAGGTAGCGCAC
N-SH2 of GAP	sense	TCCCCCGGGGTGGTATCACGGAAAACTTGACAGAACG
	antisense	TGCGGTCGACTCAAACTGGGTAAAGTAATTTTTCTCC
C-SH2 of GAP	sense	TCCCCCGGGGTGGTTCCATGGGAAGATTTCC
	antisense	TGCGGTCGACTCATACAGGTTCCTTAAGATAATATCC

Table 2-3 Primer pairs used in this section.

β-galactosidase assay

The filter assay was performed according to the method of Bartel et al. (Bartel et al., 1993) as described in section 2-1-1.

Site-directed mutagenesis

Site-directed mutagenesis of Flt-1 and the primers used were described in section 2-1-1.

2-3-2 Results and Discussion

Nck and SHP-2 bind to Flt-1.

In section 2-2-2, we showed that Sck binds to KDR and Flt-1 cytoplasmic regions via its SH2 domain. These results indicate that SH2 domains are important for Sck binding to KDR and Flt-1 cytoplasmic regions and suggest that other proteins that have SH2 domains may also bind to KDR or Flt-1 via their SH2 domains. As described in section 2-1, the SH2 domains of PI3K p85, PLCγ, Nck and GAP have been shown to form a complex with KDR or Flt-1 upon VEGF stimulation in BAEC (Guo et al., 1995). In addition to these proteins, the bindings of three other proteins, Grb2, SHP-2 and Stat3 to Flt-1 or KDR has also been suggested (Kroll and Waltenberger, 1997). Grb2 and tyrosine phosphatase SHP-2 have been shown to bind to KDR in KDR-overexpressing porcine aortic endothelial cells in a VEGF-dependent manner (Kroll and Waltenberger, 1997). Flt-1 has the consensus motif (YXXQ) for Stat3 binding (Stahl et al., 1995) in its cytoplasmic region (YSFQ; 1002 - 1005 amino acids).

In this study, I tested the binding of SH2 domains of these proteins to KDR and Flt-1 cytoplasmic region. For this purpose, I co-expressed the cytoplasmic region of Flt-1 or KDR with the SH2 domain of each protein using the yeast two-hybrid system. In this system, reconstitution of functional transcription factor through the binding between the bait protein

and the prey protein leads to the expression of reporter gene β-galactosidase. The cytoplasmic region of Flt-1 or KDR was introduced into pGBT9 as the bait. SH2 domains of PLCγ, PI3K p85, Nck, Grb2, SHP-2, Stat3 and GAP (Fig. 2-8) were introduced into pGAD424 as preys. The resultant bait-prey plasmids were co-transformed into the yeast reporter strains, SFY526 and Y190 in various combinations. The transformants were grown on filters and their β-galactosidase activities were visualized using X-Gal as a substrate. As shown in Fig. 2-9, the N- and C-SH2 domains of PLCγ, N- and C-SH2 domains of PI3K p85, SH2 domain of Nck, and N-SH2 domain of SHP-2 bound to Flt-1. The C-SH2 domain of SHP-2 and SH2 domain of Grb2 did not bind to Flt-1. Furthermore, I could not detect the binding of SH2 domain of Stat3 and GAP to Flt-1.

The N-SH2 of PLCγ bound to KDR as previously reported (Cunningham et al., 1997) and C-SH2 domain of PLCγ also bound to KDR (Fig. 2-10). Unexpectedly, I could not detect a significant binding of SH2 domain of Grb2 nor both SH2 domains of SHP-2 to KDR, although the interaction of Grb2 and SHP-2 with KDR has been suggested (Kroll and Waltenberger, 1997). This discrepancy might be derived from the weak binding of KDR to prey proteins with SH2 domain in the yeast two-hybrid system used in this study. Actually, previous studies showed that the magnitude of binding between KDR and N-SH2 domain of PLCγ is relatively weak in comparison to Flt-1 (Cunningham et al., 1997).

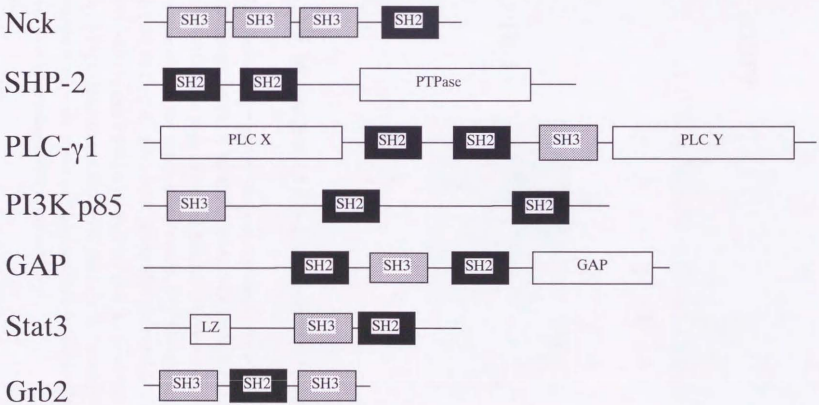

Fig. 2-8 SH2 containg proteins used in this study.

Fig. 2-9 Interaction of Flt-1 with certain SH2 domains.

The cytoplasmic region of Flt-1 was introduced into pGBT9 as a bait. The SH2 domains of PLCγ, PI3K p85, Stat3, Nck, Grb2, SHP-2 were introduced into pGAD424 as preys. Resultant bait and prey plasmids were co-transformed into the yeast reporter strains, SFY526 [pGAD424 (a), PLCγ N-SH2 (b), PLCγ C-SH2 (c), PI3K p85 N-SH2 (d), PI3K p85 C-SH2 (e) and Stat3 SH2 (f)] and Y190 [pGAD424 (g), Nck (h), Grb2 (i), SHP-2 N-SH2 (j), SHP-2 C-SH2 (k) and SHP-2 NC-SH2 (l)] in various combinations. Transformants were grown on filters and their b-galactosidase activities were visualized using X-Gal as substrate.

Fig. 2-10 Interaction of KDR with certain SH2 domains.

The cytoplasmic region of KDR was introduced into pGBT9 as a bait. The SH2 domains of PLCg, PI3K p85, Stat3, Nck, Grb2, SHP-2 were introduced into pGAD424 as preys. Resultant bait and prey plasmids were co-transformed into the yeast reporter strains, SFY526 [pGAD424 (a), PLCγ N-SH2 (b), PLCγ C-SH2 (c), PI3K p85 N-SH2 (d), PI3K p85 C-SH2 (e) and Stat3 SH2 (f)] and Y190 [pGAD424 (g), Nck (h), Grb2 (i), SHP-2 N-SH2 (j), SHP-2 C-SH2 (k) and SHP-2 NC-SH2 (1)] in various combinations. Transformants were grown on filters and their b-galactosidase activities were visualized using X-Gal as substrate.

Furthermore, I could not detect the binding of SH2 domains of PI3K p85, Stat3 nor GAP to KDR (data for GAP are not shown). Taken together, these results indicate that Nck and SHP-2 may directly bind to Flt-1.

Nck binds to Y1213 and Y1333 of Flt-1

To determine the tyrosine residues of Flt-1 responsible for Nck binding, I co-transformed the SH2 domain of Nck and Flt-1 mutant constructs whose tyrosine residues were individually mutated to phenylalanine (Fig. 2-6). β-galactosidase activity of each transformant was quantified using Galacton-Star as a substrate. As shown in Fig. 2-11, mutation of the kinase domain (K861F) resulted in a complete loss of the enzyme activity. Substitution of Y1213 resulted in 93% loss of β-galactosidase activity, while substitution of Y1333 resulted in 89% loss. Interestingly, substitution of Y1242 resulted in 321% gain in activity for unknown reasons. These results indicated that two tyrosine residues of Flt-1, Y1213 and Y1333, are responsible for binding to the SH2 domain of Nck.

Y1213 is followed by VNA, and Y1333 is followed by STP. The results do not agree with Y-D-E-P/D/V, the preferred sequence for Nck SH2 domain binding determined in *in vitro* phosphopeptide studies (Songyang et al., 1993).

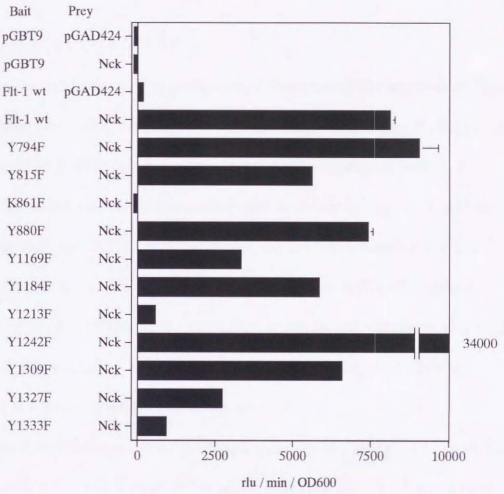

Fig. 2-11 Interactions of Nck SH2 with mutant constructs of Flt-1 cytoplasmic region.

Liquid assay of β-galactosidase activities expressed in yeast host Y190 using chemiluminescent Galacton Star as substrate. Values represent the mean ±SD of triplicate determinations expressed in relative light units divided by reaction time (60 min) and optical density.

SHP-2 binds to Y1213 of Flt-1

In the next series of experiments, I determined the residues of Flt-1 responsible for SHP-2 binding. I co-transformed Flt-1 mutants described above and the N-SH2 domain or N- and C-SH2 domains of SHP-2. β-galactosidase activity of each transformant is shown in Fig. 2-12 and the result showed that Y1213 of Flt-1 might be the major binding site for SHP-2. Substitution of Y1213 resulted in 95% loss of β-galactosidase activity. Y1213 is followed by VNA. As the preferred sequence of SHP-2 N-SH2 domain binding is Y-V/I/T-X-V/L/I (Songyang et al., 1993), Y1213VNA almost matched with the sequence.

As determined previously (Cunningham et al., 1995), Y1213 of Flt-1 is responsible for PI3-kinase p85 binding (data not shown). I also found that Y1169 of Flt-1 is responsible for such binding (data not shown).

In summary, I showed in this section, using the yeast two hybrid system, that Nck may bind to Y1213 and Y1333 of Flt-1 and that SHP-2 may bind to Y1213 of Flt-1. Considering that Y1213 of Flt-1 has been shown to be the binding site for PI3K p85 (Cunningham et al., 1995) and is autophosphorylated when Flt-1 was expressed in both yeast and insect cells (Cunningham et al., 1995; Sawano et al., 1997), Y1213 of Flt-1 may be autophosphorylated upon the binding of VEGF and become a target for certain SH2-containing proteins, for example, PI3K p85, Nck and SHP-2.

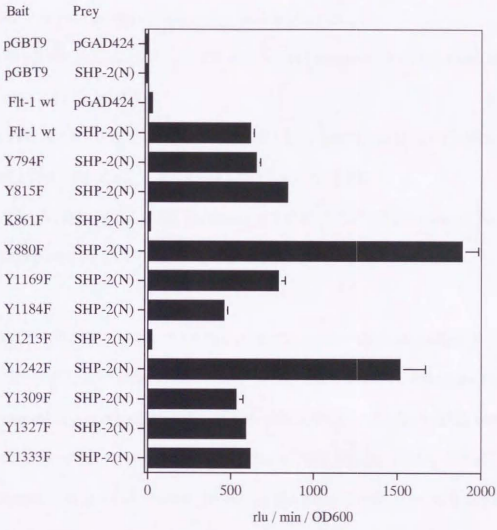

Fig.2-12 Interactions of SHP-2 SH2 with Flt-1 cytoplasmic region mutant constructs.

Liquid assay of β-galactosidase activities expressed in yeast host Y190 using chemiluminescent Galacton Star as substrate. Values represent the mean ± SD of triplicate determinations expressed in relative light units divided by reaction time (60 rain) and optical density.

Table 2-4 summarizes the results of this chapter.

(1) Both the SH2 domain of Sck and N-SH2 domain of PLCγ bind to the same site, Y1175, of KDR.

(2) The N-SH2 and C-SH2 domains of PLCγ and N-SH2 and C-SH2 domains of PI3K p85 bind to the same site, Y1169, of Flt-1.

(3) The N-SH2 and C-SH2 domains of PI3K p85, SH2 domain of Nck and N-SH2 domain of SHP-2 bind to the same site, Y1213, of Flt-1.

These results prompted us to compare the amino acid sequences of SH2 domains that bind to the same sites of KDR and Flt-1. As shown in Fig. 2-13, the homology score of the alignment of Sck SH2 to PLCγ N-SH2 was 79 (maximum possible score: 461) while that of Nck SH2 to SHP-2 N-SH2 was 165 (maximum possible score: 369). On the other hand, that of Sck SH2 to Shc SH2 was 342 (maximum possible score: 461). Therefore, the homology between Sck SH2 and PLCγ N-SH2 is low and that between Nck SH2 and SHP-2 N-SH2 is medium. These results suggest that the three-dimensional structures of Sck SH2 and PLCγ N-SH2 are somewhat different and that inhibition of binding of Sck SH2 to Y1175 of KDR without inhibition of binding of PLCγ N-SH2 to KDR might be possible. Further structural analysis is important to determine the above conclusion.

		KDR		Flt-1	
		binding	site	binding	site
Sck	PTB	-		-	
	SH2	+	Y1175 YIVLP	+	?
PLCγ	N-SH2	+	Y801* YLSIV	+	Y794* YLSII
			Y1175 YIVLP		Y1169*† YIPIN
	C-SH2	±	?	-	
PI3K p85	N-SH2	+	ND	+	Y1169 YIPIN
					Y1213** YVNAF
	C-SH2	-		+	Y1169 YIPIN
					Y1213** YVNAF
Nck	SH2	-		+	Y1213 YVNAF
					Y1333 YSTPP
SHP-2	N-SH2	-		+	Y1213 YVNAF
	C-SH2	-		-	
Grb2	SH2	-		-	
GAP	SH2	-		-	
Stat3	SH2	-		-	

Table 2-4 Summary of the results

+ significant binding

- no detectable binding

* Cunningham et al., 1997

**Cunningham et al., 1995

† Sawano et al., 1997

A

```
                10        20        30        40        50        60        70        80        90
                *   *   *   *   *   *   *   *   *   *   *   *   *   *   *   *   *   *   *   *
Sck SH2     WYHGRMSRRAAERMLRADGDFLVRDSVTNPGQYVLTGMHAGQPKHLLLVDPEGVVRTKDVLFESISHLIDHHLQNGQPIVAAESELHLRGVVSR
                ||||:|||||| |  |||:||  |:|| |||   | :|: ||:||||||| |||:|: ||  ||  :| ||||
PLCγ N-SH2  _______________pDGsFLVReSeTfvGdYtLsfwrnGkvqHihsrqdaGtpkTdnlvFdSlydLItHy-Qqv-PlrcnEfEmrL>

Maximum possible score:     461
homology score:             79
```

B

```
                10        20        30        40        50        60        70
                *   *   *   *   *   *   *   *   *   *   *   *   *   *   *
Nck SH2     WYYGKVTRHQAEMALNERGHEGDFLIRDSESSPNDFSVSLKAQGKNKHFKVQLKETVYCIGQRKFSTMEELVEHYKKA
            ||: |||  |||  | :|| ||:|| | |:|||:||||||| ||  :|||| ::: | ||  |||||:||||:|
SHP-2 N     WfhpniTgveAEnllltRGvdGsFLaRpSkSnPgDFtlSvrrnGavtHiKiQntgdyYdlGgeKFaTlaELVqyY>

Maximum possible score:     396
homology score:             165
```

C

```
                10        20        30        40        50        60        70        80        90
                *   *   *   *   *   *   *   *   *   *   *   *   *   *   *   *   *   *   *   *
Sck SH2     WYHGRMSRRAAERMLRADGDFLVRDSVTNPGQYVLTGMHAGQPKHLLLVDPEGVVRTKDVLFESISHLIDHHLQNGQPIVAAESELHLRGVVSR
            |||||||||:|| ||| |||||||||:|:|||||||||||||||||||||||||||||||  ||||||||::||||  |||||:||| ||  |:|
Shc SH2     WfHGklSRReAEalLqlnGDFLVReStTtPGQYVLTGlqsGQPKHLLLVDPEGVVRTKDhrFESvSHLIsyHmdNhlPIisAgSELcLqqpVeR>

Maximum possible score:     461
homology score:             342
```

Fig. 2-13 Alignment of SH2 regions

Identical or closely related amino acids are marked with vertical lines.
(A) Alignment of Sck SH2 to PLCγ N-SH2
(B) Alignment of Nck SH2 to SHP-2 N-SH2
(C) Alignment of Sck SH2 to Shc SH2

Chapter 3

Screening for inhibitors of VEGF binding to its receptor KDR

3-1 Introduction

In Chapter 2, I described the results of my studies on protein binding to KDR and Flt-1 cytoplasmic regions.

In this chapter, using the second strategy described in the introduction of this thesis (Chapter One), I describe the results of screening for inhibitors of VEGF binding to its receptor KDR.

I selected KDR as the main target for the inhibitors of VEGF binding to its receptors. KDR has a stronger tyrosine kinase activity than Flt-1 and several studies have indicated that KDR plays a more important role in VEGF signal transduction than Flt-1 (Seetharam et al., 1995). In studies using porcine aortic endothelial cells (PAEC), which express very small amounts of KDR and Flt-1, stimulation of KDR induces various cellular responses. In comparison, stimulation of Flt-1 induces only MAPK and a weak DNA synthesis but does not induce chemotaxis (Landgren E et al., 1998; Seetharam et al., 1995).

The assay system utilizing I^{125}-VEGF is commonly used for the detection of VEGF binding to KDR (Gitay-Goren et al., 1996; Keyt et al., 1996; Soker et al., 1996). In this method, I^{125}-VEGF is first incubated with cells expressing KDR. After several washes, the amount of the bound VEGF is quantified by measuring the radioactivity of I^{125}-VEGF. Since it provides

quantitative data, this method is very useful. However, it inevitably produces radioactive waste, and therefore, this method is not suitable for mass screening.

As an alternative approach, I first developed a non-radioactive method for the detection of VEGF binding to KDR. Using VEGF with FLAG epitope at its amino terminus, I developed the ELISA system, in which VEGF binding to KDR is detected with an anti-FLAG antibody (Fig. 3-1).

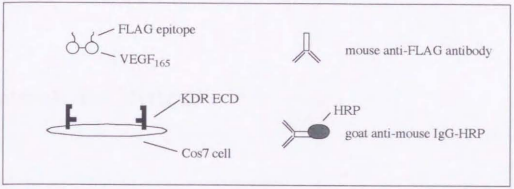

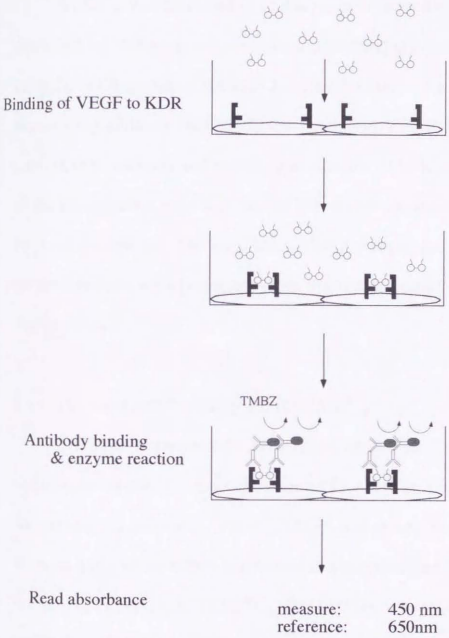

Fig. 3-1 Procedure used for detecting VEGF binding to KDR using FLAG-VEGF ELISA.

FLAG-VEGF is first incubated with KDR ECD transfected COS-7 cells for 2hrs. After extensive washes, cells are incubated with anti-FLAG antibody for 1hr. After extensive washes, cells are incubated with HRP-conjugated anti-mouse IgG for 1hr. After extensive washes,HRP activity is revealed with TMBZ as a substrate.

3-2 Materials and Methods

Materials

$VEGF_{165}$ was produced in *Pichia pastoris* according to the method described by Mohanraj and coworkers (Mohanraj et al., 1995) and purified using Ni-NTA column (QIAGEN Inc., Santa Clara, CA). Anti-VEGF neutralizing antibody (MAB293) was purchased from R & D Systems, Inc. Anti-MAPK antibody and anti-phospho specific MAPK antibody were part of the PhosphoPlus MAPK Antibody Kit, which was purchased from New England Biolabs Inc. (Beverly, MA). TMBZ was purchased from Sumilon. Other chemicals were purchased from Specs & Biospecs, Maybridge or Sigma/Aldrich.

Expression and purification of FLAG-$VEGF_{165}$

The yeast N-terminal FLAG Expression system (Eastman Chemical Company) was used for the expression of FLAG-$VEGF_{165}$ in *Saccharomyces cerevisiae*. $VEGF_{165}$ cDNA was cloned by PCR using human placenta quick-clone cDNA (Clontech) as a template and VEGF/FW (CCGAATTCATGAACTTTCTGCTGTCTTG), VEGF/RV (GGGGATCCTCACCGCCTCGGCTTGTCACA) as primers. The amplified DNA fragment was digested with *Eco*RI, *Bam*HI and subcloned into *Eco*RI, *Bam*HI pre-digested YEpFLAG-1. The clone

carrying $VEGF_{165}$ cDNA was confirmed by sequencing. The plasmid (YEpFLAG-$VEGF_{165}$) was introduced into *S. cerevisiae* BJ3505 strain and transformants were selected for growth without tryptophan. Transformants were incubated in 10 mL of Trp-medium overnight at 30°C. The overnight culture was added to 200 mL YPEM medium (1% dextrose, 3% glycerol, 1% yeast extract, 2% peptone) and incubated at 30°C for 48 hr. The supernatant was collected by centrifugation and 5.6 mL 10 × TBS / Ca (0.5 M Tris, pH 7.4, 1.5 M NaCl, and 100 mM $CaCl_2$) was added to it. The mixture was loaded onto the anti-FLAG M1 Affinity column (Eastman Chemical Company), and the protein was eluted with 2 mL TBS / EDTA (TBS containing 2 mM EDTA). The eluate was dialyzed overnight with TBS. The purity of FLAG-$VEGF_{165}$ was about 90%, as determined by SDS-PAGE. The amount of FLAG-$VEGF_{165}$ was 40 μg, as determined by VEGF ELISA (R & D Systems, Inc.).

Detection of binding of FLAG-$VEGF_{165}$ to KDR or Flt-1 in COS-7 cells by ELISA.

The extracellular regions, including transmembrane domain of KDR (1~806 amino acids) and Flt-1 (1~800 amino acids) were amplified by PCR. The templates were KDR and Flt-1 cDNA (kindly provided by Dr. M. Shibuya, Department of Genetics, Institute of Medical Science, University of Tokyo). The primer pairs were KDRFW

(GGGAATTCCCACCATGGAGAGCAAGGTGCTGCT), KDRRV (CCGAATTCTCACATGACGATGGACAAGTAGC) for KDR and FLTFW (GGGAATTTCCCACCARGGRCAGCRACRGGGACAC), FLTRV (CCGAATTCTCAGGTCCATTATAATTGATAGG) for Flt-1. The amplified DNA fragments were digested with *EcoR*I and subcloned into *EcoR*I pre-digested $pCXN_2$. The clones were confirmed by sequencing. Each plasmid (KDR / $pCXN_2$ and Flt-1 / $pCXN_2$) was transfected into COS-7 cells by Trans IT (Mirus Corporation). Transfected cells were seeded in gelatin-coated 96-well plates at a density of 5×10^4 cells per well and grown for 24 h at 37°C. Plates were washed three times with TBST (TBS containing 0.1% Tween-20) and incubated with FLAG-$VEGF_{165}$ (3 nM) in the absence or presence of inhibitors in the binding buffer (DMEM, 0.15% gelatin, and 20 mM Hepes [pH 7.4]) for 2 h at room temperature. After three washes with TBST, cells were incubated with anti-FLAG M1 antibody in the binding buffer (1: 1000) for 1 h at room temperature. After three washes with TBST, cells were incubated with anti-mouse IgG antibody conjugated to HRP (Santa Cruz, Santa Cruz, CA) in the binding buffer (1: 1000) for 1 h at room temperature. After three washes with TBST, HRP activity was revealed with TMBZ as a substrate. After 10 to 15 min, the reaction was stopped with 2 N sulfuric acid, and optical density was read at 450 nm with an ELISA plate reader.

Analysis of MAPK tyrosine phosphorylation in HUVEC.

HUVEC (primary culture, passage number less than 5 [Kurabou]) were seeded in gelatin-coated 6-well plates at a density of 3×10^5 cells per well in HuMedia-EG2 (Kurabou) and grown for 24 h at 37°C. After further incubation in the endothelial SFM medium (Life Technologies, Inc.) for 20 h, various amounts of VEGF as indicated in the legend of Fig. 4 were added to cells, followed by incubation for 3 to 10 min at 37°C. Cells were then fixed with 10% TCA for 30 min on ice and scraped. Cell lysates were prepared with 40 μL of urea solution (9 M urea, 2% Triton X-100, 1% 2-mercaptoethanol) and 10 μL of 10% SDS. Cell lysates were separated by 12% SDS-PAGE and transferred to nitrocellulose membranes. After transfer, the membranes were incubated in blocking buffer (TBS + 5% BSA) overnight at 4°C. The membranes were probed with the appropriate antibodies, anti-MAPK (1: 1000) or anti-phospho-specific MAPK antibody (1:1000), followed by HRP-conjugated anti-rabbit IgG antibody using the protocol recommended by the manufacturer. Immunoreactivity was detected by chemiluminescence (LumiGLO, New England Biolabs) and photographed with the Instant-Film Format Camera Luminometer (Tropix).

3-3 Results

Construction of a simple ELISA system to detect $VEGF_{165}$ binding to KDR.

To detect $VEGF_{165}$ binding to KDR, $VEGF_{165}$ with an N-terminal FLAG epitope (FLAG-$VEGF_{165}$) was produced in *S. cerevisiae* and used to detect its binding by ELISA with anti-FLAG antibody. $VEGF_{165}$ cDNA was subcloned into the yeast expression vector YEpFLAG-1 in order to add a FLAG epitope to its N-terminal. The resultant plasmid (YEpFLAG-$VEGF_{165}$) was introduced into *S. cerevisiae* BJ3505 strain. The FLAG-$VEGF_{165}$ protein secreted into YPEM medium was purified by anti-FLAG antibody affinity chromatography. SDS-PAGE analysis demonstrated that the eluted protein migrated as a single band under reducing conditions (Fig. 3-2). The apparent molecular weight estimated from its mobility on the gel was approximately 22 kDa (reducing conditions) and 44 kDa (non-reducing conditions). These bands were detected by both anti-VEGF antibody and anti-FLAG antibody (data not shown). The half-maximal concentration of FLAG-$VEGF_{165}$ for stimulation of DNA synthesis of HUVEC was 50 pM, (Fig. 3-3) which was similar to that of $VEGF_{165}$ (D'Angelo et al., 1995).

The KDR extracellular region (1~806 amino acids) (Terman et al., 1992) was subcloned into the mammalian expression vector $pCXN_2$, and the resulting plasmid was transfected transiently into COS-7 cells. Transfected COS-7 cells were first incubated with 3 nM FLAG-$VEGF_{165}$

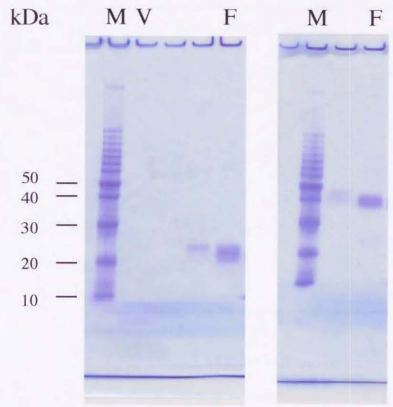

Fig. 3-2 SDS-PAGE analysis of FLAG-VEGF$_{165}$

Cultures of yeast containing YEpFLAG-VEGF$_{165}$ were purified by anti-FLAG antibody and analyzed by SDS-PAGE.
Left: non-reducing condition, *right*: reducing condition.
M lane: 10 kDa ladder molecular weight marker.
V lane: culture of yeast with empty vector.
F lane: culture of yeast with YEpFLAG-VEGF$_{165}$

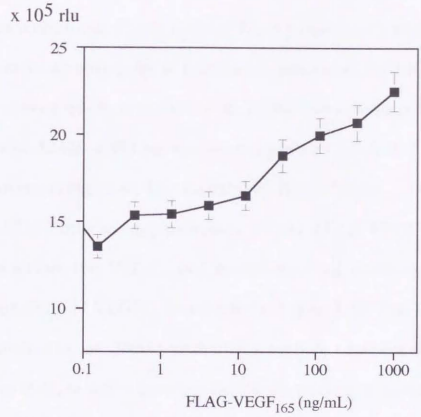

Fig. 3-3 Mitogenic effect of FLAG-VEGF $_{165}$ on HUVEC

HUVEC were seeded into a growth medium at 3 x 10^4 cells/well of 96-well plate precoated with gelatin and incubated for 24 hours. The medium was then replaced with serum-free medium for another 24 hours. Cells were stimulated with various amounts of FLAG-VEGF$_{165}$ for 16 hours. BrdU was added and cells were incubated for 8 hours. The incorporated BrdU was quantified with anti-BrdU antibody with chemiluminescent substrate. Relative light unit (rlu) was plotted against the dose of FLAG-VEGF $_{165}$.

for 2 h, then with an anti-FLAG antibody for 1 h, and finally with an anti-mouse IgG antibody conjugated to horseradish peroxidase for 1 h. The peroxidase activity was then revealed with TMBZ as a colorimetric substrate. Absorbance at 450 nm was increased in a FLAG-$VEGF_{165}$ dose-dependent manner (Fig. 3-4). The Kd value of FLAG-$VEGF_{165}$ for transfected COS-7 cells was approximately 0.5 nM. FLAG-$VEGF_{165}$ binding was inhibited by $VEGF_{165}$ and the half-maximal inhibitory concentration (IC_{50}) of $VEGF_{165}$ was about 5 nM (Fig. 3-5). This binding was also inhibited by anti-VEGF neutralizing antibody (data not shown) and suramin (Fig. 3-6), which is known to inhibit the binding of several growth factors to their receptors (Danese et al., 1993; Hosang, 1985; Johannes et al., 1996; Kloen et al., 1994).

These results indicated that FLAG-$VEGF_{165}$ bound to the KDR extracellular region expressed in COS-7 cells and that its binding can be detected employing a non-radioactive method by ELISA using an anti-FLAG antibody.

Screening for Inhibitors

Using my ELISA system, I screened my chemical libraries for compounds that might inhibit the binding of $VEGF_{165}$ to KDR. I identified 8-(3-oxo-4, 5, 6-trihydroxy-3h-xanthen-9-yl) -1- naphthoic acid (OTXNA,

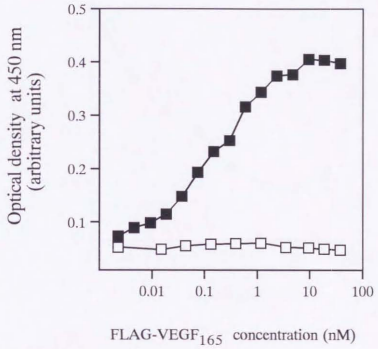

Fig. 3-4 Detection of FLAG-$VEGF_{165}$ binding to KDR expressed in COS-7 cells.

COS-7 cells transiently expressing KDR extracellular region (■) or control COS-7 cells (□) were first incubated with various amounts of FLAG-$VEGF_{165}$ for 2 hr. FLAG-$VEGF_{165}$ was detected as indicated in (3-2 MATERIALS AND METHODS).
Enzymatic activity was revealed with TMBZ as a chromogenic substrate (absorption at 450 nm). Data represent the mean ±SD of three measurements.

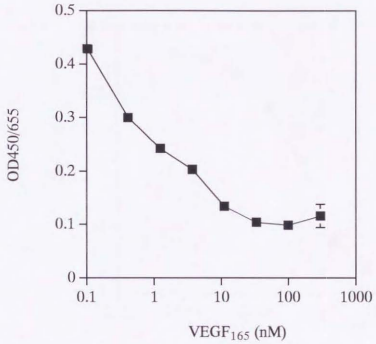

Fig. 3-5 Competition of FLAG-$VEGF_{165}$ binding to KDR expressed in COS-7 cells by $VEGF_{165}$.

Various amounts of $VEGF_{165}$ were first incubated with FLAG-$VEGF_{165}$ for 10 min. The mixture was then added to COS-7 cells transiently expressing KDR extracellular region (■) and incubated for 2 hrs. FLAG-$VEGF_{165}$ was detected as indicated in (3-2 MATERIALS AND METHODS). Enzymatic activity was revealed with TMBZ as a chromogenic substrate (absorption at 450 nm). Data represent the mean ±SD of three measurements.

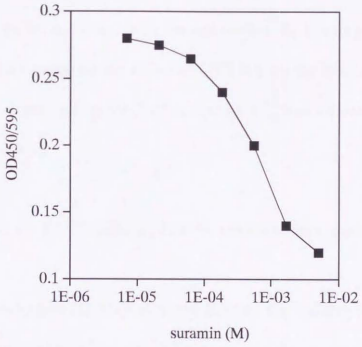

Fig. 3-6 Competition of FLAG-VEGF$_{165}$ binding to KDR expressed in COS-7 cells by suramin.

Various amounts of suramin were first incubated with FLAG-VEGF$_{165}$ for 10 min. The mixture was then added to COS-7 cells transiently expressing KDR extracellular region (■) and incubated for 2 hrs. FLAG-VEGF$_{165}$ was detected as indicated in (3-2 MATERIALS AND METHODS). Enzymatic activity was revealed with TMBZ as a chromogenic substrate (absorption at 450 nm). Data represent the mean ±SD of three measurements.

Fig. 3-7) as an inhibitor of $VEGF_{165}$ binding to KDR with an IC_{50} value of 700 μM (Fig. 3-8). Comparison of the inhibitory effect of some analogues showed that pyrogallol red (Fig. 3-7) did not inhibit the binding even at 4 mM (Fig. 3-9). I also assayed the effect of OTXNA on the binding of $VEGF_{165}$ to Flt-1 expressed in cos-7 cells, and its IC_{50} was similar to that to KDR (data not shown).

Effect of OTXNA on VEGF-induced MAPK tyrosine phosphorylation in HUVEC.

To clarify whether OTXNA directly inhibits the binding of $VEGF_{165}$ to KDR, I investigated the effect of OTXNA on $VEGF_{165}$-induced tyrosine phosphorylation of MAPK in HUVEC. MAPK tyrosine phosphorylation was revealed by anti-phospho specific MAPK antibody. Stimulation of HUVEC with $VEGF_{165}$ increased MAPK tyrosine phosphorylation after 3 min (Fig. 3-10) in a VEGF dose-dependent manner (Fig. 3-11) as reported previously (D'Angelo et al., 1995). Various amounts of OTXNA were first incubated with 0.1 nM VEGF, and mixtures were added to HUVEC for 3 min. OTXNA inhibited MAPK phosphorylation, with an IC_{50} value of 13.7 μM (Fig. 3-12).

OTXNA

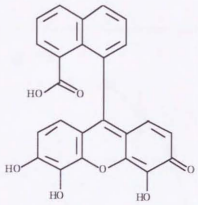

pyrogallol red

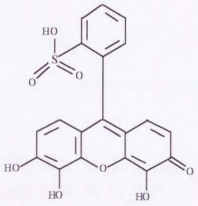

Fig. 3-7 Structures of OTXNA and pyrogallol red

OTXNA represents

8-(3-oxo-4, 5, 6-trihydroxy-3h-xanthen-9-yl) -1- naphthoic acid

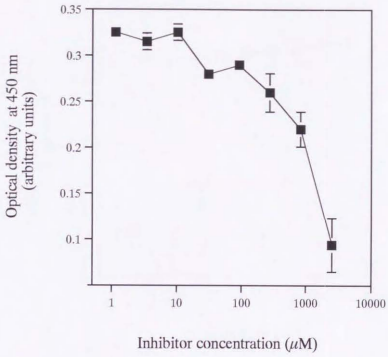

Fig. 3-8 Effect of OTXNA on the binding of FLAG-$VEGF_{165}$ to KDR expressed in COS-7 cells.

Various amounts of OTXNA were first incubated with FLAG-$VEGF_{165}$ for 30 min. The mixture was then added to COS-7 cells transiently expressing KDR extracellular region (■) and incubated for 2 hrs. FLAG-$VEGF_{165}$ was detected as indicated in (3-2 MATERIALS AND METHODS). Enzymatic activity was revealed with TMBZ as a chromogenic substrate (absorption at 450 nm).
Data represent the mean ±SD of three measurements.

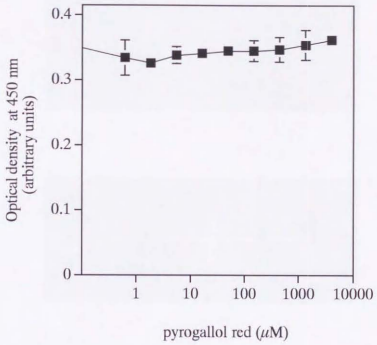

Fig. 3-9 Effect of pyrogallol red on the binding of FLAG-$VEGF_{165}$ to KDR expressed in COS-7 cells.

Various amounts of pyrogallol red were first incubated with FLAG-$VEGF_{165}$ for 30 min. The mixture was then added to COS-7 cells transiently expressing KDR extracellular region (■) and incubated for 2 hrs. FLAG-$VEGF_{165}$ was detected as indicated in (3-2 MATERIALS AND METHODS). Enzymatic activity was revealed with TMBZ as a chromogenic substrate (absorption at 450 nm). Data represent the mean ±SD of three measurements.

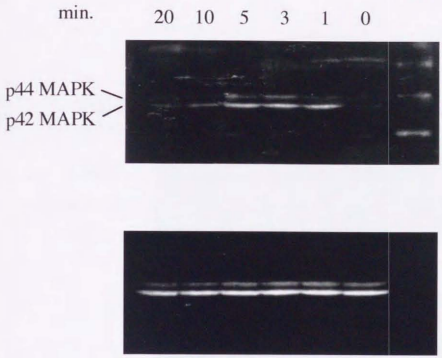

Fig. 3-10 Time course of $VEGF_{165}$-induced MAPK phosphorylation in HUVEC

Serum-starved HUVEC were stimulated with 0.1 nM of $VEGF_{165}$ for the indicated time periods. MAPK tyrosine phosphorylation was analyzed by western blotting with anti-phospho MAPK antibody (*upper panel*) or anti-MAPK antibody (*lower panel*).

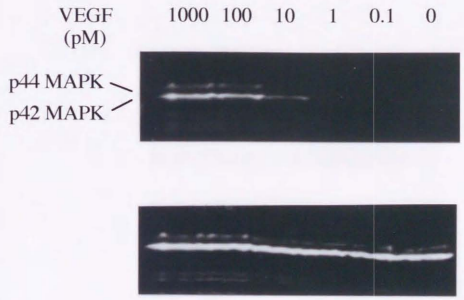

Fig. 3-11 VEGF165-dose dependent induction of MAPK phosphorylation in HUVEC

Serum-starved HUVECs were stimulated with various amounts of $VEGF_{165}$ for 3 minutes. MAPK tyrosine phosphorylation was analysed by western blotting with anti-phospho MAPK antibody *(upper panel)* or anti-MAPK antibody *(lower panel)*.

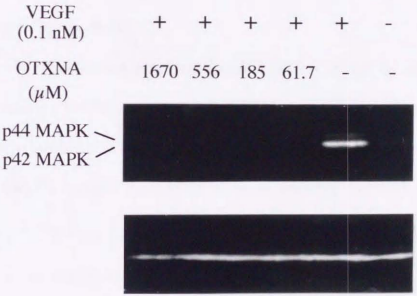

Fig. 3-12 Effect of OTXNA on $VEGF_{165}$-induced MAPK phosphorylation in HUVEC

Serum-starved HUVECs were stimulated with 0.1 nM of $VEGF_{165}$ in the presence of various amounts of OTXNA for 3 min. MAPK tyrosine phosphorylation was analysed by western blotting with anti-phospho MAPK antibody *(upper panel)* or anti-MAPK antibody *(lower panel)*.

Effect of OTXNA on bFGF- or EGF-induced MAPK tyrosine phosphorylation in HUVEC.

I next investigated the effect of OTXNA on bFGF- or EGF-induced MAPK tyrosine phosphorylation in HUVEC to determine whether OTXNA specifically inhibits the binding of $VEGF_{165}$ to KDR. bFGF and EGF induced MAPK tyrosine phosphorylation of HUVEC after 10 min as reported previously (D'Angelo et al., 1995) (Fig. 3-13). Unexpectedly, PDGF did not induce MAPK tyrosine phosphorylation even at 3 nM (data not shown).

40 μM OTXNA was incubated with bFGF, EGF or $VEGF_{165}$ for 10 min. Each mixture was then added to HUVEC for 10 min, and MAPK phosphorylation was detected by anti-phospho MAPK antibody. OTXNA inhibited $VEGF_{165}$- or bFGF-stimulated MAPK tyrosine phosphorylation, but it did not inhibit EGF-stimulated reaction (Fig. 3-14).

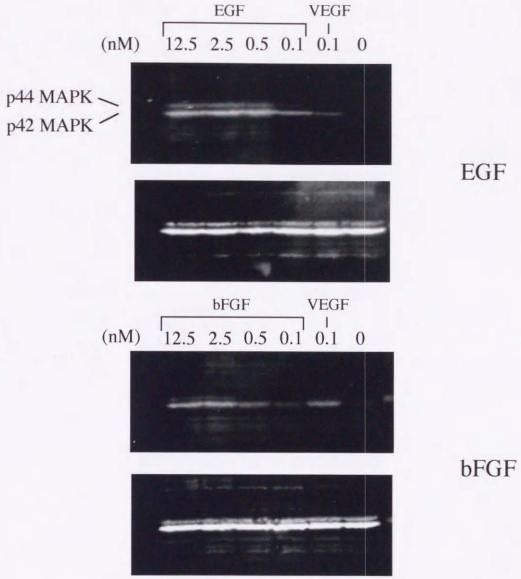

Fig. 3-13 EGF and bFGF induce MAPK phosphorylation in HUVEC

Serum-starved HUVECs were stimulated with various amounts of EGF and bFGF for 10 minutes. MAPK tyrosine phosphorylation was analysed by western blotting with anti-phospho MAPK antibody *(upper panel)* or anti-MAPK antibody *(lower panel)*.

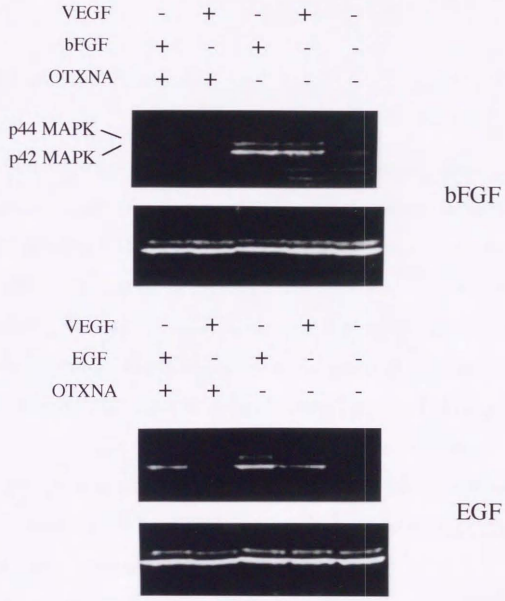

Fig. 3-14 Effect of OTXNA on MAPK phosphorylation in HUVEC induced by bFGF or EGF.

40 μM OTXNA was first incubated with 0.1 nM $VEGF_{165}$, 2.5 nM bFGF or 0.5 nM EGF for 10 min and the mixture was added to serum-starved HUVEC for 10 min. MAPK tyrosine phosphorylation was analyzed by western blotting with anti-phospho MAPK antibody *(upper panel)* or anti-MAPK antibody *(lower panel)*.

3-4 Discussion

I have shown in this study the expression of biologically active FLAG-$VEGF_{165}$ using the yeast expression system and detected its binding to KDR expressed in COS-7 cells by ELISA. The addition of FLAG peptide to the $VEGF_{165}$ N terminal did not reduce its biological activity compared with $VEGF_{165}$ with regard to their mitogenic activity and binding to KDR. The sensitivity of my ELISA system was similar to that of the binding assay using iodinated VEGF (Gitay-Goren et al., 1992). Using my ELISA system, I identified 8-(3-oxo-4, 5, 6-trihydroxy-3H-xanthen-9-yl) -1- naphthoic acid (OTXNA) with inhibitory activity against $VEGF_{165}$ binding to KDR or Flt-1 expressed in COS-7 cells. My results indicate that the novel ELISA system is useful to identify antagonists of VEGF.

My results also showed that OTXNA inhibited $VEGF_{165}$- and bFGF-induced MAPK phosphorylation in HUVEC, but it did not inhibit EGF-induced MAPK phosphorylation. These results suggest that inhibition of OTXNA of $VEGF_{165}$ or bFGF-induced MAPK phosphorylation is not due to the cellular toxicity of OTXNA. The binding of $VEGF_{165}$ to KDR or Flt-1 and bFGF to FGFRs may have common features that differ from the binding of EGF to EGFR and OTXNA may affect such common features. The structures of VEGF and bFGF are different (Moy et al., 1996; Muller et al., 1997), while the extracellular regions of KDR (Terman et al., 1992),

Flt-1 and bFGFR (Lee et al., 1989) have a common feature, i.e., Ig-like domains, although the same region of EGFR does not have an Ig-like domain (Ullrich et al., 1984) (Fig. 3-15). The second Ig-like domain of KDR or Flt-1 is essential for the binding of $VEGF_{165}$ to these receptors (Davis-Smith et al., 1996). Both Ig-like domains 2 and 3 of FGF receptors are essential for the binding of basic FGF to the receptor (Zimmer et al., 1993). Therefore, I suspect that OTXNA might bind to Ig-like domains of KDR, Flt-1 or FGFR. However, further studies are required to confirm the inhibitory mechanism of OTXNA.

$VEGF_{165}$ and bFGF are heparin-binding growth factors (Saksela et al., 1988; Tessler et al., 1994), and the presence of heparin-like molecules is essential for the binding of both factors to their receptors (Gitay-Goren et al., 1992; Rapraeger et al., 1991; Yayon et al., 1991). Therefore, heparin might be involved in the inhibitory mechanism of OTXNA. However, suramin, which inhibits the binding of growth factors to heparin-like molecules, inhibits not only the binding of $VEGF_{165}$ and bFGF but also that of EGF to their receptors (Danese et al., 1993; Hosang, 1985; Johannes et al., 1996; Kloen et al., 1994). These data indicate that OTXNA-induced inhibition may not be related to heparin.

The IC_{50} value of OTXNA for the binding of $VEGF_{165}$ to KDR was about 700 μM and that for $VEGF_{165}$-induced MAPK tyrosine phosphorylation in HUVEC was 13.7 μM. For the binding assay, 3 nM

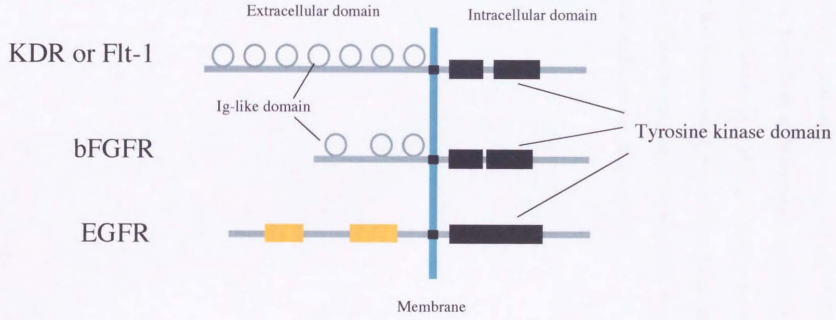

Fig. 3-15 Comparison of VEGFRs, bFGFR and EGFR

KDR, Flt-1 and bFGFR have Ig-like domains in their extracellular domains.
On the other hand, EGFR does not have Ig-like domains.

FLAG-$VEGF_{165}$ was used, but only 0.1 nM $VEGF_{165}$ was used for MAPK activation. Therefore, a higher concentration of OTXNA might be required to inhibit the binding of $VEGF_{165}$ to KDR in my ELISA assay.

OTXNA would be a seed compound for the development of VEGF specific inhibitors. I plan to investigate the inhibitory mechanism of OTXNA in more detail and improve its specificity.

Chapter Four

Novel indications for application of the yeast two-hybrid system for screening of VEGF signal transduction inhibitors

4-1 Introduction

In Chapter 2, I showed the results of analysis of KDR and Flt-1 binding proteins. I identified Sck as a new binding protein to KDR and Flt-1. I also showed that Nck and SHP-2 bind to Flt-1. The role of Sck in VEGF signal transduction was not, however, determined. I believe that Sck is one of the most important targets for VEGF inhibitors.

However, to identify small molecules that inhibit VEGF signal transduction at protein-protein interaction level, I have to construct an excellent screening method that allows accurate assay of a large number of samples within a short period of time.

The possible application of the yeast two-hybrid system for identification of small molecule inhibitors of protein-protein interactions was suggested by Fields and Sternglanz (Fields and Sternglanz, 1994). In the original yeast two-hybrid system, protein-protein interaction in yeasts leads to the expression of a reporter gene *HIS3*, which permits the yeast to grow without histidine. Therefore, small molecule inhibitors of protein-protein interactions can be selected as growth inhibitors of the yeast in a histidine-free medium (Fig. 4-1). However, this principle is impractical itself because growth inhibitors, such as protein synthesis inhibitors, DNA synthesis inhibitors and respiration inhibitors, would also be selected in the actual screening and are difficult to be excluded.

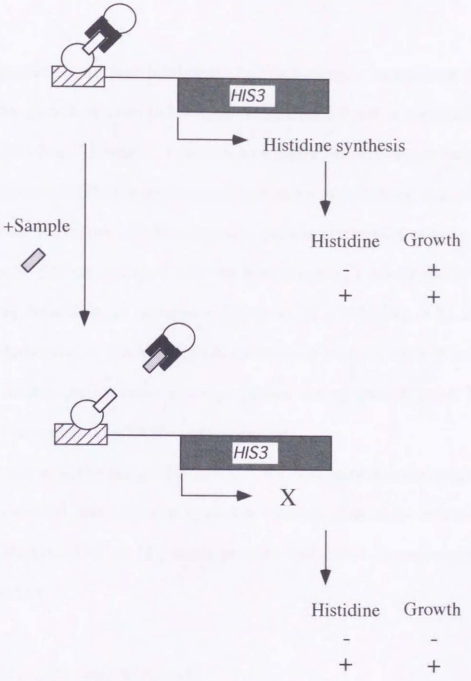

Fig. 4-1 Application of the yeast two-hybrid system for screening of small molecular inhibitors of protein-protein interactions.

Yeast containing the target proteins grows in histidine-free medium. Inhibitors of protein-protein interactions should inhibit yeast growth in histidine-free medium.

I predicted that true inhibitors of protein-protein interactions should inhibit the growth of yeast in histidine-free media but not in media that contain histidine. Therefore, I defined ΔI% index, the difference between percent growth inhibition without histidine and with histidine, as a new index of the inhibitory activity of protein-protein interaction of test compounds. The feasibility of ΔI% has been previously confirmed by evaluating the activity of ascomycin (Kawai et al., 1993) (Fig. 4-2), an FK506-derivative, which binds to FK506 binding protein (FKBP) and thereby inhibits the interaction of type I transforming growth factor beta (TGF-β) receptors with FKBP.

In this chapter, using ΔI% as my index, I showed that the original yeast two-hybrid system can be applied as a simple method for selecting small molecule inhibitors of protein-protein interactions, for example, KDR and Sck.

4-2 Materials and Methods

Yeast two-hybrid system

The original yeast two-hybrid system was purchased from Clontech. cDNAs of ALK5 and FKBP (Wang et al., 1996) were cloned by PCR using human leukocyte cDNA library as a template and their sequences were confirmed by DNA sequencing. The cytoplasmic domain of ALK5 was PCR

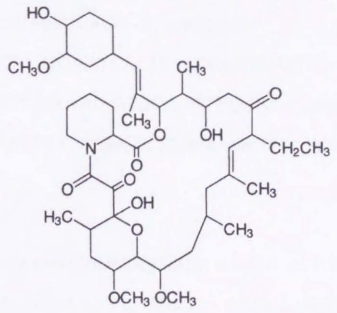

Fig. 4-2 Structure of ascomycin

Ascomycin is an ethyl analog of FK506 with similar immunosuppressant properties (Kawai et al., 1993).

amplified, subcloned into pGBT9 and used as the bait plasmid. The full-length FKBP was PCR amplified, subcloned into pGAD424 and used as the prey plasmid. Primer pairs were: sense 5' - GGAATTCCGACGGAGGCAGG -3', antisense 5'-ACGCGTCGACCTATTGAATCACTTTAGGCTTCTCTGG -3' for ALK5. sense 5' - GGAATTCATGGGAGTGCAGGTGGAA - 3', antisense 5' - CCGCTCGAGTTATCATTCCAGTTTTAGAAGCTCC - 3' for FKBP.

Assay procedure

Yeast reporter strain PJ69-2A (*MATa, ura3-52, his3-200, trp1-901, leu2-3, 112, gal4Δ, gal80Δ, LYS2 :: GAL1*$_{UAS}$*-GAL1*$_{TATA}$*-HIS3, GAL2*$_{UAS}$*-GAL2*$_{TATA}$*-ADE2)* was transformed with designated plasmid. Resultant transformants were seeded in 2 ml SD/-LW medium (yeast nitrogen base 0.67%, glucose 2%, various nutrients without leucine and tryptophan) and incubated at 30°C overnight. After washing twice with SD/-LWH (yeast nitrogen base 0.67%, glucose 2%, various nutrients without leucine, tryptophan and histidine), cells were diluted to optical density of 0.1 with SD/-LW or SD/-LWH and 200 μl of the diluted cultures were placed into wells of 96-well culture plates. Various concentrations of ascomycin were added to the wells and the plates were incubated at 30°C for 72 hour. The optical density of the culture was read at 600 nm with the microplate reader

and $\Delta I\%$ index of each concentration of ascomycin was calculated as indicated in Results and Discussion.

4-3 Results and Discussion

ΔI%, a new index of the inhibitory activity of protein-protein interaction of the sample compound, was calculated using the following formula:

ΔI%=I%(-H) - I%(+H)

where:

I% = 100 × [OD(-sample) - OD(+sample)] / OD(-sample)

OD = optical density at 600 nm

-H = histidine-free medium

+H = medium containing histidine

ΔI% represents the inhibitory activity of each sample on *HIS3*-dependent growth of the yeast and consequently, it represent the inhibitory activity of the sample on protein-protein interaction.

I tested whether ΔI% is a useful index by evaluating the inhibitory activity of ascomycin, an FK506-derivative (Fig. 4-2), on the interaction of ALK5 with FKBP. The cytoplasmic region of ALK5 was fused to the DNA binding domain of Gal4 and full-length FKBP was fused to the transcriptional activating domain of Gal4. Resultant plasmids were co-transformed into the yeast PJ69-2A. As a control, a plasmid for expressing the full length Gal4 was transformed into the same strain. First, the growth

of transformants in histidine-free conditions was confirmed. Optical density of the yeasts rose in an incubation time-dependent manner (data not shown). In the next step, the activity of ascomycin was quantified using ΔI%. Ascomycin was added at various concentrations to the yeast culture and incubated for 72 hr at 30°C. Optical density of the culture was measured with a 96 well microplate reader. ΔI% was calculated and plotted with the concentration of ascomycin. As shown in Fig. 4-3, ΔI% rose in dose-dependent manner with a maximum of 64% when the yeast co-transformed with ALK5 and FKBP was used. The half-maximal effective concentration of ascomycin was 200 nM. On the other hand, ΔI% was almost zero when the yeast transformed with Gal4 was used. Fig. 4-4 shows ΔI% of cycloheximide was almost zero with both yeasts, indicating that general growth inhibitors, such as cycloheximide, may inhibit the growth of yeast with or without histidine and therefore results in low ΔI% value. Taken together, I conclude that the inhibitory activity of protein-protein interactions of test samples can be semi-quantified with the yeast two-hybrid system using the ΔI% index.

In the actual screening using ΔI%, Gal4 function inhibitors and His3 activity inhibitors would also be selected. These false positives would be excluded as those that inhibit histidine-free growth of the yeast transformed with Gal4. True positives, such as ascomycin, should have considerably

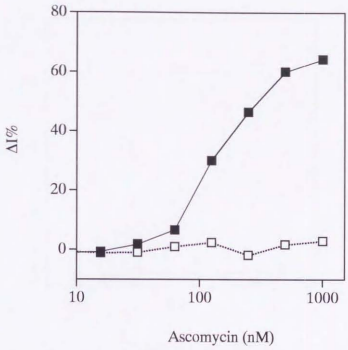

Fig. 4-3. Inhibitory effect of ascomycin on interaction between ALK5 and FKBP.

Cultures of yeast PJ69-2A transformed with Ga14 DB-ALK5 and Ga14 TA-FKBP (■) or control yeast PJ69-2A transformed with Ga14 full-length (□) were suspended in media with or without histidine and transferred into wells of 96-well plates. Various concentrations of ascomycin were added to the wells and incubated at 30°C for 72 hr. Optical density at 600 nm was read with a microplate reader. Ordinate: ΔI% of each ascomycin concentration.

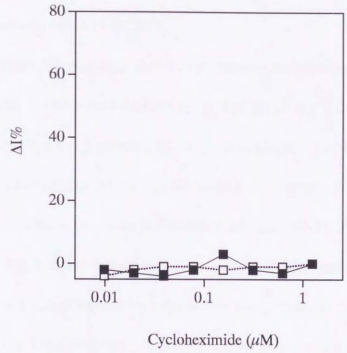

Figure 4-4. Effect of cycloheximide on ΔI%.

Cultures of yeast PJ69-2A transformed with Ga14 DB-ALK5 and Ga14 TA-FKBP (■) or control yeast PJ69-2A transformed with Ga14 full length (□) were suspended in media with histidine or without histidine and transferred into wells of 96-well plates. Various concentrations of cycloheximide were added to the wells and incubated at 30°C for 72 hr. Optical density at 600 nm was read with a microplate reader. Ordinate: DI% of each cycloheximide concentration.

high ΔI% with the yeast expressing the target proteins but low ΔI% with the yeast expressing Gal4 (Fig. 4-3).

Recently, Huang and Schreiber (Huang and Schreiber, 1997) reported the inducible reverse two-hybrid assay for selecting small molecule inhibitors of protein-protein interactions. In that assay, the protein-protein interaction in yeast leads to the expression of a reporter gene *URA3*, which converts 5-fluoroorotic acid (5-FOA) to a toxic substance. Therefore, small molecules with protein-protein interaction inhibitory activities would be selected as those that recover the growth of the yeast in 5-FOA-containing media. Growth inhibitors would inhibit yeast growth and therefore be excluded. The feasibility of that assay system has been demonstrated in that FK506 recovers the growth of yeast expressing TGF beta receptor I and FKBP in 5-FOA-containing media. The system is excellent in that the true positive samples are selected as those that recover yeast growth. However, there are two unfavorable properties associated with the use of the above test for mass screening, these include the cost-effectiveness and rather complex operation. The above system requires 5-FOA, a comparatively expensive material in assay media. In addition, it requires a change of sugar material from glucose to galactose in order to express target proteins. On the other hand, the original two-hybrid system used in my study requires no extra materials or change of sugar.

Using ΔI% as an index of the inhibitory activity of the test sample, I have shown in this study that the original two-hybrid system is applicable to screen for small molecule inhibitors of protein-protein interactions. ΔI% is potentially a powerful index for the actual screening of VEGF signal transduction inhibitors.

Chapter 5

Conclusions and Future Directions

In this study, I took a step toward the development of new anti-angiogenesis drugs that specifically inhibit VEGF activity. As a first step, I screened for KDR binding proteins using the yeast two-hybrid system, and identified Sck, a Shc homologue (Nakamura et al., 1998), and its binding to Y1175 of KDR receptor via its SH2 domain. Sck has the consensus sequence for the binding of Grb2 in its CH domain, and it has been shown that it is phosphorylated in EGF signal transduction (Nakamura et al., 1998). These data strongly suggest that Sck is involved in VEGF signal transduction. In future studies, I plan to investigate the roles of Sck in VEGF signal transduction, i.e., whether it is phosphorylated upon VEGF stimulation and whether it is necessary for VEGF-induced growth stimulation. Such efforts will clearly show whether Sck is a suitable target for VEGF inhibitors. I have identified other clones that bind to KDR, which are not homologous to known proteins. There may be targets among these that are more promising than Sck. This topic is now under investigation.

Next, I analyzed the binding of SH2-containing proteins to KDR and Flt-1 receptors to determine the potential targets for inhibitors of VEGF signal transduction. The results showed that Nck, an adapter protein, binds to Y1213 and Y1333 of Flt-1 and that SHP-2, protein tyrosine phosphatase, binds to Y1213 of Flt-1 via its amino terminus SH2 domain. Considering that PI3K p85 binds to Y1213 of Flt-1, the latter may be the multiple signaling protein binding site of Flt-1 and the most important site for Flt-1

downstream signal transduction. These data prompt me to develop small molecules that mimic the structure of the amino acid sequence around Y1213 of Flt-1 and inhibit the binding of important signaling proteins to Flt-1.

I also identified OTXNA, an inhibitor of VEGF binding to KDR, by screening using my ELISA system with FLAG-VEGF. Indeed, the inhibitory activity of OTXNA is insufficient and its specificity is not very high for inhibition of the cellular response induced by bFGF as well as VEGF. However, by investigating the structure-activity relationship (SAR) of OTXNA, I believe that I can improve both its inhibitory activity and specificity. The data showing that pyrogallol red, an analogue of OTXNA, did not inhibit VEGF binding to KDR may be helpful for further improvement of OTXNA. In addition to improvement of OTXNA, I have to continue screening for other compounds with a stronger activity and higher specificity than OTXNA.

I also investigated the usefulness of a new screening system for small molecule inhibitors of the protein-protein interaction. The results showed that $\Delta I\%$ is a useful index when the original yeast two-hybrid system is used for screening. Using the $\Delta I\%$ index, a simple assay system to estimate the activity of the test sample could be constructed. This assay system requires only the incubation of samples in yeast culture for two or three days. Therefore, I believe that this system is suitable as first choice method to be

used for mass screening. It may also be suitable for the high through put screening using assay robots and I have indeed already confirmed in my laboratory that the test could be applied as an automated assay.

Thus, I have established the seed compound for inhibitors of VEGF binding to KDR receptor and few targets for inhibition of VEGF intracellular signal transduction. I also tested and confirmed the suitability of a new method for the screening of VEGF signal transduction inhibitors. Based on the study outlined in this dissertation, I believe that the development of clinically effective VEGF inhibitors should become possible near future. At that stage, the effectiveness of such compounds against tumor growth should be tested in animals and humans.

References

Abedi, H., and Zachary, I. (1997) Vascular endothelial growth factor stimulates tyrosine phosphorylation and recruitment of new focal adhesions of focal adhesion kinase and paxillin in endothelial cells. J. Biol. Chem. 272, 15442-15451.

Aiello, L. P., Avery, R. L., Arrigg, P. G., Keyt, B. A., Jampel, H. D., Shah, S. T., Pasquale, L. R., Thieme, H., Iwamoto, M. A., Park, J. E., and et al. (1994) Vascular endothelial growth factor in ocular fluid of patients with diabetic retinopathy and other retinal disorders. N. Engl. J. Med. 331, 1480-1487.

Arbiser, J. L., Moses, M. A., Fernandez, C. A., Ghiso, N., Cao, Y., Klauber, N., Frank, D., Brownlee, M., Flynn, E., Parangi, S., Byers, H. R., and Folkman, J. (1997) Oncogenic H-ras stimulates tumor angiogenesis by two distinct pathways. Proc. Natl. Acad. Sci. U S A 94, 861-866.

Bartel, P. L., Chien, C.-T., Sternglanz, R., and Fields, S. (1993) Using the two-hybrid system to detect protein-protein interactions. Cellular Interactions in Development: A Practical Approach., 153-179.

Berkman, R. A., Merrill, M. J., Reinhold, W. C., Monacci, W. T., Saxena, A., Clark, W. C., Robertson, J. T., Ali, I. U., and Oldfield, E. H. (1993) Expression of the vascular

permeability factor/vascular endothelial growth factor gene in central nervous system neoplasms. J. Clin. Invest. 91, 153-159.

Berse, B., Brown, L. F., Van de Water, L., Dvorak, H. F., and Senger, D. R. (1992) Vascular permeability factor (vascular endothelial growth factor) gene is expressed differentially in normal tissues, macrophages, and tumors. Mol. Biol. Cell. 3, 211-220.

Brown, L. F., Berse, B., Jackman, R. W., Tognazzi, K., Manseau, E. J., Dvorak, H. F., and Senger, D. R. (1993) Increased expression of vascular permeability factor (vascular endothelial growth factor) and its receptors in kidney and bladder carcinomas. Am. J. Pathol. 143, 1255-1262.

Connolly, D. T., Olander, J. V., Heuvelman, D., Nelson, R., Monsell, R., Siegel, N., Haymore, B. L., Leimgruber, R., and Feder, J. (1989) Human vascular permeability factor. Isolation from U937 cells. J. Biol. Chem. 264, 20017-20024.

Cunningham, S. A., Arrate, M. P., Brock, T. A., and Waxham, M. N. (1997) Interactions of FLT-1 and KDR with phospholipase C gamma: identification of the phosphotyrosine binding sites. Biochem. Biophys. Res. Commun. 240, 635-639.

Cunningham, S. A., Waxham, M. N., Arrate, P. M., and Brock, T. A. (1995) Interaction of the Flt-1 Tyrosine Kinase Receptor with the p85 Subunit of Phosphatidylinositol 3-Kinase. J. Biol. Chem. 270, 20254-20257.

D'Angelo, G., Struman, I., Martial, J., and RI, W. (1995) Activation of mitogen-activated protein kinases by vascular endothelial growth factor and basic fibroblast growth factor in capillary endothelial cells is inhibited by the antiangiogenic factor 16-kDa N-terminal fragment of prolactin. Proc. Natl. Acad. Sci. USA 92, 6374-6378.

Danese, R., Del Bianchi, S., Soldani, P., Campagni, A., La Rocca, R., Myers, C., Paparelli, A., and Del Tacca, M. (1993) Suramin inhibits bFGF-induced endothelial cell proliferation and angiogenesis in the chick chorioallantoic membrane. Br. J. Cancer 68, 932-938.

Davis-Smith, T., Chen, H., Park, J., Presta, L. G., and Ferrara, N. (1996) The second immunoglobulin-like domain of the VEGF tyrosine kinase receptor Flt-1 determines ligand binding and may initiate a signal transduction cascade. EMBO J. 15, 4919-4927.

de Vries, C., Escobedo, J. A., Ueno, H., Houck, K., Ferrara, N., and Williams, L. T. (1992) The fms-like tyrosine kinase, a receptor for vascular endothelial growth factor. Science 255, 989-991.

Dvorak, H. F., Sioussat, T. M., Brown, L. F., Berse, B., Nagy, J. A., Sotrel, A., Manseau, E. J., Van de Water, L., and Senger, D. R. (1991) Distribution of vascular permeability factor (vascular endothelial growth factor) in tumors: concentration in tumor blood vessels. J. Exp. Med. 174, 1275-1278.

Ferrara, N. (1995) The role of vascular endothelial growth factor in pathological angiogenesis. Breast Cancer Res. Treat. 36, 127-137.

Ferrara, N., and Davis-Smyth, T. (1997) The biology of vascular endothelial growth factor. Endocrine Reviews 18, 4-25.

Ferrara, N., and Henzel, W. J. (1989) Pituitary follicular cells secrete a novel heparin-binding growth factor specific for vascular endothelial cells. Biochem. Biophys. Res. Commun. 161, 851-858.

Fields, S., and Sternglanz, R. (1994) The two-hybrid system: an assay for protein-protein interactions. Trends. Genet. 10, 286-292.

Folkman, J. (1995) Angiogenesis in cancer, vascular, rheumatoid and other disease. Nature Medicine 1, 27-31.

Folkman, J., (1996) Fighting Cancer by Attacking Its Blood Supply. SCIENTIFIC AMERICAN *September* (Nikkei Scicence (1996) 12, p.160-163)

Fong, G. H., Rossant, J., Gertsenstein, M., and Breitman, M. L. (1995) Role of the Flt-1 receptor tyrosine kinase in regulating the assembly of vascular endothelium. Nature 376, 66-70.

Gitay-Goren, H., Cohen, T., Tessler, S., Soker, S., Gengrinovitch, S., Rockwell, P., Klagsbrun, M., Levi, B. Z., and Neufeld, G. (1996) Selective binding of VEGF121 to

one of the three vascular endothelial growth factor receptors of vascular endothelial cells. J. Biol. Chem. 271, 5519-5523.

Gitay-Goren, H., Soker, S., Vlodavsky, I., and Neufeld, G. (1992) The binding of vascular endothelial growth factor to its receptors is dependent on cell surface-associated heparin-like molecules. J. Biol. Chem. 267, 6093-6098.

Guo, D., Jia, Q., Song, H. Y., Warren, R. S., and Donner, D. B. (1995) Vascular endothelial cell growth factor promotes tyrosine phosphorylation of mediators of signal transduction that contain SH2 domains. Association with endothelial cell proliferation. J. Biol. Chem. 270, 6729-6733.

Hori, A., Sasada, R., Matsutani, E., Naito, K., Sakura, Y., Fujita, T., and Kozai, Y. (1991) Suppression of solid tumor growth by immunoneutralizing monoclonal antibody against human basic fibroblast growth factor. Cancer Res. 51, 6180-6184.

Hosang, M. (1985) Suramin binds to platelet-derived growth factor and inhibits its biological activity. J. Cell. Biochem. 29, 265-273.

Huang, J., and Schreiber, S. L. (1997) A yeast genetic system for selecting small molecule inhibitors of protein-protein interactions in nanodroplets. Proc. Natl. Acad. Sci. USA 94, 13396-13401.

Igarashi, K., Isohara, T., Kato, T., Shigeta, K., Yamano, T., and Uno, I. (1998) Tyrosine 1213 of Flt-1 Is a Major Binding Site of Nck and SHP-2. Biochem. Biophys. Res. Commun. 246, 95-99.

Johannes, W., Ulrike, M., Hedwig, F., and Vinzenz, H. (1996) Suramin is a potent inhibitor of vascular endothelial growth factor. A contribution to the molecular basis of its antiangiogenic action. J. Mol. Cell Cardiol. 28, 1523-1529.

Kawai, M., Lane, B. C., Hsieh, G. C., Mollison, K. W., Carter, G. W., and Luly, J. R. (1993) Structure-activity profiles of macrolactam immunosuppressant FK-506 analogues. FEBS Lett. 316, 107-113.

Keck, P. J., Hauser, S. D., Krivi, G., Sanzo, K., Warren, T., Feder, J., and Connolly, D. T. (1989) Vascular permeability factor, an endothelial cell mitogen related to PDGF. Science 246, 1309-1312.

Keyt, B. A., Berleau, L. T., Nguyen, H. V., Chen, H., Heinsohn, H., Vandlen, R., and Ferrara, N. (1996) The carboxyl-terminal domain (111-165) of vascular endothelial growth factor is critical for its mitogenic potency. J. Biol. Chem. 271, 7788-7795.

Kieser, A., Weich, H. A., Brandner, G., Marme, D., and Kolch, W. (1994) Mutant p53 potentiates protein kinase C induction of vascular endothelial growth factor expression. Oncogene 9, 963-969.

Kim, K. J., Li, B., Winer, J., Armanini, M., Gillett, N., Phillips, H. S., and Ferrara, N. (1993) Inhibition of vascular endothelial growth factor-induced angiogenesis suppresses tumour growth *in vivo*. Nature 362, 841-844.

Kloen, P., Jennings, C., Gebhardt, M., Springfield, D., and Mankin, H. (1994) Suramin inhibits growth and transforming growth factor-beta1(TGF-beta 1) binding in osteosarcoma cell lines. Eur. J. Cancer 30A, 678-682.

Kodama, R., Takahashi, K., and Shibuya, M. (1997) Vascular Biology. Kodansha 193.

Kondo, S., Asano, M., and Suzuki, H. (1993) Significance of vascular endothelial growth factor/vascular permeability factor for solid tumor growth, and its inhibition by the antibody. Biochem. Biophys. Res. Commun. 194, 1234-1241.

Kroll, J., and Waltenberger, J. (1997) The vascular endothelial growth factor receptor KDR activates multiple signal transduction pathways in porcine aortic endothelial cells. J. Biol. Chem. 272, 32521-32527.

Landgren E, Schiller P, Cao Y, and L, C.-W. (1998) Placenta growth factor stimulates MAP kinase and mitogenicity but not phospholipase C-gamma and migration of endothelial cells expressing Flt 1. Oncogene 16, 359-367.

Lee, P., Johnson, D., Cousens, L., Fried, V., and Williams, L. (1989) Purification and complementary DNA cloning of a receptor for basic fibroblast growth factor. Science 245, 57-60.

Leung, D. W., Cachianes, G., Kuang, W. J., Goeddel, D. V., and Ferrara, N. (1989) Vascular endothelial growth factor is a secreted angiogenic mitogen. Science 246, 1306-1309.

Mauceri, H. J., Hanna, N. N., Beckett, M. A., Gorski, D. H., Staba, M. J., Stellato, K. A., Bigelow, K., Heimann, R., Gately, S., Dhanabal, M., Soff, G. A., Sukhatme, V. P., Kufe, D. W., and Weichselbaum, R. R. (1998) Combined effects of angiostatin and ionizing radiation in antitumour therapy. Nature 394, 287-291.

Millauer, B., Longhi, M. P., Plate, K. H., Shawver, L. K., Risau, W., Ullrich, A., and Strawn, L. M. (1996) Dominant-negative inhibition of Flk-1 suppresses the growth of many tumor types *in vivo*. Cancer Res. 56, 1615-1620.

Millauer, B., Shawver, L. K., Plate, K. H., Risau, W., and Ullrich, A. (1994) Glioblastoma growth inhibited *in vivo* by a dominant-negative Flk-1 mutant. Nature 367, 576-579.

Mohanraj, D., Olson, T., and Ramakrishnan, S. (1995) Expression of biologically active human vascular endothelial growth factor in yeast. Growth Factors 12, 17-27.

Moy, F. J., Seddon, A. P., Bölen, P., and Powers, R. (1996) High-resolution solution structure of basic fibroblast growth factor determined by multidimensional heteronuclear magnetic resonance spectroscopy. Biochemistry *35*, 13552-13561.

Muller, Y. A., Li, B., Christinger, H. W., Wells, J. A., Cunningham, B. C., and De Vos, A. M. (1997) Vascular endothelial growth factor: Crystal structure and functional mapping of the kinase domain receptor binding site. J. Biol. Chem. *94*, 7192-7197.

Nakamura, T., Muraoka, S., Sanokawa, R., and Mori, N. (1998) N-Shc and Sck, two neuronally expressed shc adapter homologs. J. Biol. Chem. *273*, 6960-6967.

Pe'er, J., Shweiki, D., Itin, A., Hemo, I., Gnessin, H., and Keshet, E. (1995) Hypoxia-induced expression of vascular endothelial growth factor by retinal cells is a common factor in neovascularizing ocular diseases. Lab. Invest. *72*, 638-645.

Peters, K. G., De Vries, C., and Williams, L. T. (1993) Vascular endothelial growth factor receptor expression during embryogenesis and tissue repair suggests a role in endothelial differentiation and blood vessel growth. Proc. Natl. Acad. Sci. U S A *90*, 8915-8919.

Pfeffer, L. M., Mullersman, J. E., Pfeffer, S. R., Murti, A., Shi, W., and Yang, C. H. (1997) STAT3 as an adapter to couple phosphatidylinositol 3-kinase to the IFNAR1 chain of the type I interferon receptor. Science *276*, 1418-1420.

Pierce, G. F., Tarpley, J. E., Yanagihara, D., and et al. (1992) Platelet-derived growth factor (BB homodimer), transforming growth factor-β1, and basic fibroblast growth factor in dermal wound healing. Am. J. Pathol. *140*, 1375-1388.

Plate, K. H., Breier, G., Weich, H. A., and Risau, W. (1992) Vascular endothelial growth factor is a potential tumour angiogenesis factor in human gliomas *in vivo*. Nature *359*, 845-848.

Quinn, T. P., Peters, K. G., De Vries, C., Ferrara, N., and Williams, L. T. (1993) Fetal liver kinase 1 is a receptor for vascular endothelial growth factor and is selectively expressed in vascular endothelium. Proc. Natl. Acad. Sci. U S A *90*, 7533-7537.

Rapraeger, A. C., Krufka, A., and Olwin, B. B. (1991) Requirement of heparan sulfate for bFGF-mediated fibroblast growth and myoblast differentiation. Science *252*, 1705-1708.

Robinson, G. S., Pierce, E. A., Rook, S. L., Foley, E., Webb, R., and Smith, L. E. (1996) Oligodeoxynucleotides inhibit retinal neovascularization in a murine model of proliferative retinopathy. Proc. Natl. Acad. Sci. U S A *93*, 4851-4856.

Saksela, O., D. Moscatelli, A. Sommer, and Rifkin, D. B. (1988) Endothelial cell-derived heparan sulfate binds basic fibroblast growth factor and protects it from proteolytic degradation. J. Cell Biol. *107*, 743-751.

Sawano, A., Takahashi, T., Yamaguchi, S., and Shibuya, M. (1997) The Phosphorylated 1169-Tyrosine Containing Region of Flt-1 Kinase (VEGFR-1) Is a Major Binding Site for PLCγ. Biochem. Biophys. Res. Commun. *238*, 487-491.

Seetharam, L., Gotoh, N., Maru, Y., Neufeld, G., Yamaguchi, S., and Shibuya, M. (1995) A unique signal transduction from FLT tyrosine kinase, a receptor for vascular endothelial growth factor VEGF. Oncogene *10*, 135-147.

Shalaby, F., Rossant, J., Yamaguchi, T. P., Gertsenstein, M., Wu, X. F., Breitman, M. L., and Schuh, A. C. (1995) Failure of blood-island formation and vasculogenesis in Flk-1-deficient mice. Nature *376*, 62-66.

Shibuya, M. (1995) Role of VEGF-flt receptor system in normal and tumor angiogenesis. Adv. Cancer Res. *67*, 281-316.

Shweiki, D., Itin, A., Soffer, D., and Keshet, E. (1992) Vascular endothelial growth factor induced by hypoxia may mediate hypoxia-initiated angiogenesis. Nature *359*, 843-645.

Soker, S., Fidder, H., Neufeld, G., and Klagsbrun, M. (1996) Characterization of novel vascular endothelial growth factor (VEGF) receptors on tumor cells that bind VEGF165 via its exon 7-encoded domain. J. Biol. Chem. *271*, 5761-5767.

Soker, S., Takashima, S., Miao, H. Q., Neufeld, G., and Klagsbrun, M. (1998) Neuropilin-1 is expressed by endothelial and tumor cells as an isoform-specific receptor for vascular endothelial growth factor. Cell *92*, 735-745.

Songyang, Z., Shoelson, S. E., Chaudhuri, M., Gish, G., Pawson, T., Haser, W. G., King, F., Roberts, T., Ratnofsky, S., and Lechleider, R. J., et al (1993) SH2 domains recognize specific phosphopeptide sequences. Cell *72*, 767-778.

Stahl, N., Farruggella, T. J., Boulton, T. G., Zhong, Z., Darnell, J. E. J., and Yancopoulos, G. D. (1995) Choice of STATs and Other Substrates Specified by Modular Tyrosine-Based Motifs in Cytokine Receptors. Science *267*, 1349-1353.

Takahashi, A., Sasaki, H., Kim, S. J., Tobisu, K., Kakizoe, T., Tsukamoto, T., Kumamoto, Y., Sugimura, T., and Terada, M. (1994) Markedly increased amounts of messenger RNAs for vascular endothelial growth factor and placenta growth factor in renal cell carcinoma associated with angiogenesis. Cancer Res. *54*, 4233-4237.

Terman, B. I., Dougher-Vermazen, M., Carrion, M. E., Dimitrov, D., Armellino, D. C., Gospodarowicz, D., and Bohlen, P. (1992) Identification of the KDR tyrosine kinase as a receptor for vascular endothelial cell growth factor. Biochem. Biophys. Res. Commun. *187*, 1579-1586.

Tessler, S., Rockwell, P., Hicklin, D., Cohen, T., Levi, B. Z., Witte, L., Lemischka, I. R., and Neufeld, G. (1994) Heparin modulates the interaction of VEGF165 with soluble and cell associated flk-1 receptors. J. Biol. Chem. *269*, 12456-12461.

Ullrich, A., Coussens, L., Hayflick, J., Dull, T., Gray, A., Tam, A., Lee, J., Yarden, Y., Libermann, T., and Schlessinger, J. (1984) Human epidermal growth factor receptor cDNA sequence and aberrant expression of the amplified gene in A431 epidermoid carcinoma cells. Nature *309*, 418-425.

Waltenberger, J., Claesson-Welsh, L., Siegbahn, A., Shibuya, M., and Heldin, C. H. (1994) Different Signal Transduction Properties of KDR and Flt1, Two Receptors for Vascular Endothelial Growth Factor. J. Biol. Chem. *269*, 26988-26995.

Wang, T., Li, B. Y., Danielson, P. D., Shah, P. C., Rockwell, S., Lechleider, R. J., Martin, J., Manganaro, T., and Donahoe, P. K. (1996) The immunophilin FKBP12 functions as a common inhibitor of the TGF beta family type I receptors. Cell *86*, 435-444.

Yayon, A., Klagsbrun, M., Esko, J. D., Leder, P., and Ornitz, D. M. (1991) Cell surface, heparin-like molecules are required for binding of basic fibroblast growth factor to its high affinity receptor. Cell *64*, 841-848.

Zetter, B. R. (1998) Angiogenesis and tumor metastasis. Annu. Rev. Med. *49*, 407-424.

Zimmer, Y., Givol, D., and Yayon, A. (1993) Multiple structural elements determine ligand binding of fibroblast growth factor receptors. Evidence that both Ig domain 2 and 3 define receptor specificity. J. Biol. Chem. *268*, 7899-7903.

(VEGF情報伝達阻害活性を有する新規血管新生抑制剤開発のための研究)

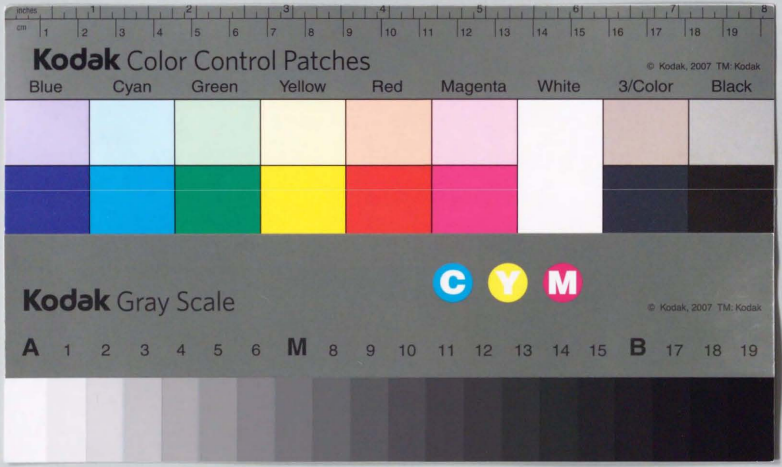
inches
cm
Kodak Color Control Patches
© Kodak, 2007 TM: Kodak
Blue
Cyan
Green
Yellow
Red
Magenta
White
3/Color
Black
Kodak Gray Scale
C
Y
M
© Kodak, 2007 TM: Kodak
A 1 2 3 4 5 6 M 8 9 10 11 12 13 14 15 B 17 18 19